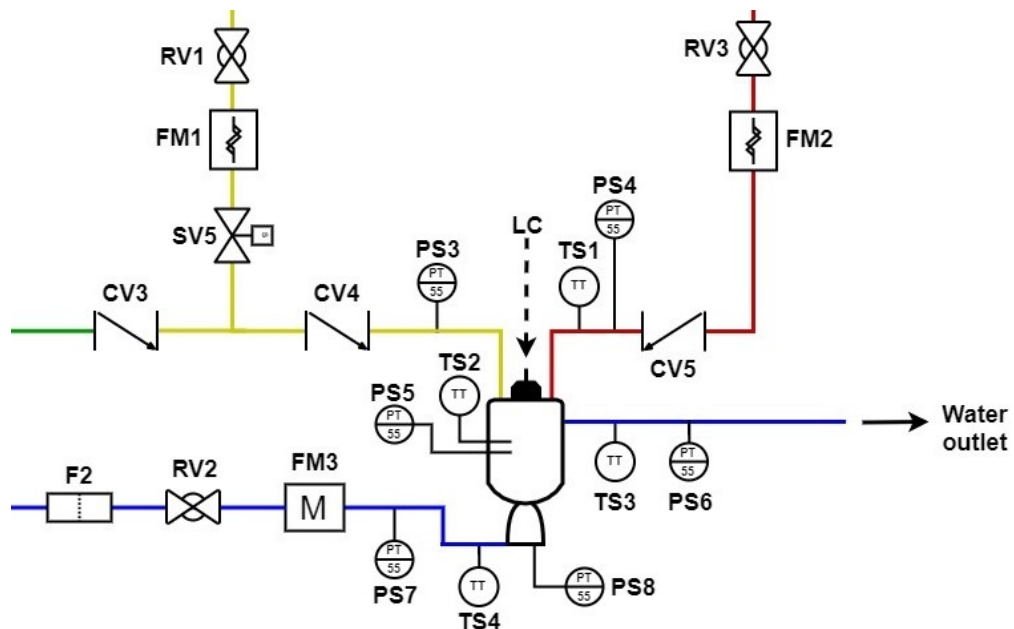


DEGREE PROJECT

L

Preliminary design of a small-scale liquid-propellant rocket engine testing platform



Erik Andersson

Space Engineering, master's level

2019

Luleå University of Technology
Department of Computer Science, Electrical and Space Engineering

LULEÅ UNIVERSITY OF TECHNOLOGY

MASTER THESIS

**Preliminary design of a small-scale
liquid-propellant rocket engine testing platform**

Author:
Erik ANDERSSON

Supervisor:
Dr. Élcio JERONIMO DE OLIVEIRA

Examiner:
Dr. Anita ENMARK

*A thesis submitted in partial fulfilment of the requirements
for the degree of Master in Space Engineering*

in the

Department of Computer Science, Electrical and Space Engineering

5th December 2019

This page intentionally left blank

LULEÅ UNIVERSITY OF TECHNOLOGY

Abstract

Department of Computer Science, Electrical and Space Engineering

Master in Space Engineering

Preliminary design of a small-scale liquid-propellant rocket engine testing platform

by Erik ANDERSSON

Propulsion system testing before mission operation is a fundamental requirement in any project. For both industrial and commercial entities within the space industry, complete system integration into a static test platform for functional and performance testing is an integral step in the system development process. Such a platform - if designed to be relatively safe, uncomplicated and reliable - can be an important tool within academia as well, giving researchers and students a possibility for practical learning and propulsion technology research.

In this thesis, a preliminary design for a liquid-propellant rocket engine testing platform to be used primarily for academical purposes is developed. Included in the presented design is a bi-propellant Chemical Propulsion system, gas pressure fed with Gaseous Nitrogen and using Gaseous Oxygen as oxidiser and a 70 % concentrated ethanol-water mixture as fuel. The propellant assembly contains all necessary components for operating the system and performing combustion tests with it, including various types of valves, tanks and sensors. An estimation of the total preliminary cost of selected components is presented as well. Also part of the developed platform design is a small thrust chamber made of copper, water-cooled and theoretically capable of delivering 1000 N of thrust using the selected propellants.

A list of operations to be performed before, during and after a complete combustion test is presented at the end of the document, together with a preliminary design of a Digital Control and Instrumentation System software. Due to time limitations, the software could not be implemented in a development program nor tested with simulated parameters as part of this thesis project.

Acknowledgements

First of all I would like to thank my supervisor, Dr. Élcio Jeronimo de Oliveira, for his immense support and guidance throughout my thesis. I would also like to thank my examiner, Dr. Anita Enmark, for her helpful input to the development of my report.

Thank you to the advisors of this project:

- Vanderlei Neias at Edge of Space, for showing me their assembled test platform and helping me with the component selections.
- Anna Lind at GKN Aerospace, for her very helpful suggestions regarding the pressure and temperature measurements of the thrust chamber.
- A special thank you to Olle Persson at Luleå Tekniska Universitet (LTU), for introducing me to this thesis project. Thank you for answering all my questions and giving me suggestions and input at all stages of the design process, on everything from safety concerns to component selections.

I of course wish to thank my family, for giving me their full support through the course of my engineering studies. I'm especially grateful to Ulf Palmnäs, for encouraging and guiding me at every step of the way. Thank you for so enthusiastically sharing with me your knowledge and your contacts, and for providing me with invaluable support during difficult times.

Lastly, to Jens Bergström and Daniel Lindh, thank you for the company and for your help during the countless report writing and late night study sessions of these past five years. The journey would have been much harder without you.

Contents

Abstract	i
Acknowledgements	ii
List of Figures	vi
List of Tables	vii
Abbreviations	viii
Physical Constants	x
List of Symbols	xi
1 Introduction	1
1.1 Project motivation	1
1.2 Objectives	2
1.3 Project management plan	2
2 Literature Review - Propulsion and Control	4
2.1 Propulsion systems	4
2.1.1 Types	5
Electric Propulsion	5
Chemical Propulsion	6
2.1.2 System comparison	7
EP vs CP	7
Solid CP vs Liquid CP	8
2.1.3 Bi-propellant liquid propulsion systems	9
Design	9
Propellants	11
2.1.4 Nozzle design	14
2.1.5 Thrust chamber cooling	15
2.2 Propulsion system testing	16
2.3 Digital Control and Instrumentation System	17
3 Theoretical Background	18
3.1 Design equations	18
3.1.1 Thrust chamber	18
Thrust and velocities	18
Propellant mass flow rates	19
Thrust chamber size	19
Chamber cooling	21
3.1.2 Propellant feed assembly	22
Pressurised tanks	22

4 Hardware Design	23
4.1 Requirements	23
4.1.1 Reasoning	23
Engine type	23
Propellants	24
Thrust chamber and cooling	24
4.1.2 List of requirements	24
4.2 Thrust chamber	25
4.2.1 Nozzle sizing	25
4.2.2 Combustion chamber sizing	27
4.2.3 Wall sizing and cooling	28
Thrust chamber and cooling jacket walls	28
Coolant water	29
4.2.4 Propellant mass flow rates and injector properties	29
4.2.5 Ignition assembly	30
4.2.6 Thrust chamber design summary	31
4.3 Propellant feed assembly	32
4.3.1 Fuel tank	34
4.3.2 Pressurised gas tanks	34
4.3.3 Plumbing	35
4.3.4 Flow control components	35
Valves	35
Pressure regulator assemblies	37
Filters	38
4.3.5 Parameter measurement components	38
Thrust	38
Mass flow rate	38
Pressure	39
Temperature	40
4.3.6 Electrical interface	40
4.4 Component costs	41
5 Software Design	43
5.1 Operations	43
5.1.1 System functionality test phase	43
5.1.2 Combustion test preparation phase	44
5.1.3 Combustion test phase	44
5.1.4 Combustion test ABORT procedure	45
5.2 Flowcharts of operations	45
5.3 Requirements	48
5.3.1 Data storage	48
5.3.2 User interface	48
Configuration screen	49
Assembly overview screen	49
Combustion test screen	49
Additional screens	50
6 Discussion and conclusions	51
6.1 Thrust chamber	51
6.2 Propellant feed assembly	51
6.3 Costs	52

6.4 Software	52
6.5 Encountered problems and design changes	52
6.5.1 Changes to propellant feed assembly structure	52
6.5.2 Component changes	53
6.6 Future work	53
6.6.1 Finalisation of testing platform	53
Software tasks	53
Hardware tasks	53
6.6.2 Improvements and future developments of finished platform	54
References	55
Appendix A Component cost table	61
Appendix B Edge of Space combustion chamber	67

List of Figures

2.1	Gas pressure fed liquid propulsion system.	11
2.2	The de Laval nozzle.	15
4.1	MATLAB plots, k value selection.	26
4.2	MATLAB plots, L_c and D_c selection.	28
4.3	Thrust chamber preliminary design drawing.	31
4.4	Propellant feed assembly schematic.	33
5.1	Flowchart of system operations.	46
5.2	Flowchart of functionality test operations.	47
B.1	Edge of Space combustion chamber.	67

List of Tables

4.1	Thrust chamber parameters.	25
4.2	Nozzle cross-sectional areas.	27
4.3	Mass flow rate parameters.	31
4.4	Summarised component costs.	42
A.1	Component costs.	61

Abbreviations

ADC	Analog to Digital Conversion
ATO	Air To Open
CD	Converging-Diverging
COTS	Commercial Off-The-Shelf
CP	Chemical Propulsion
CV	Check Valve
DAC	Digital to Analog Conversion
DAQ	Data AcQuisition
DB	Double-Base
DCIS	Digital Control and Instrumentation System
DLR	Deutsches zentrum für Luft- und Raumfahrt
DN	Diameter Nominal
D-sub	D-subminiature
ECSS	European Cooperation for Space Standardization
EFC	Ethanol Fuel Concentration
EP	Electric Propulsion
ESC	Esrangé Space Center
F	Filter
FM	Flow Meter
GOx	Gaseous Oxygen
GN2	Gaseous Nitrogen
HFOV	Horizontal Field Of View
I/O	Input/Output
IR	Infrared Radiation
ITA	Instituto Tecnológico de Aeronáutica
LC	Load Cell
LOX	Liquid O ₂ xigen
LTU	Luleå Tekniska Universitet (Luleå University of Technology)
M	Mach number
MMH	MonoMethylHydrazine
MV	Manual Valve
NFPA	National Fire Protection Association
NPT	National Pipe Thread
NTO	Nitrogen TetrOxide
PEEK	PolyEther Ether Ketone
PFA	PerFluoroalkoxy Alkane
PG	Pressure Gauge
PID	Proportional–Integral–Derivative
P&ID	Piping and Instrumentation Diagram
PRV	Pressure Relief Valve
PS	Pressure Sensor
PTFE	PolyTetraFluoroEthylene

RCV	Research Control Valves
RD	Rupture Disk
RFNA	Red Fuming Nitric Acid
RP	Rocket Propellant
RV	Regulating Valve
SSC	Swedish Space Corporation
SV	Solenoid Valve
TBD	To Be Determined
TESPEMET	TESt Platform for Electronics Modules in Electric Thrusters
TFE	TetraFluoroEthylene
TS	Temperature Sensor
UDMH	Unsymmetrical DiMethylHydrazine
VFOV	Vertical Field Of View
WF	Working Fluid

Physical Constants

Average acceleration of gravity at sea level	$g_0 = 9.81 \text{ m s}^{-2}$
Universal gas constant	$R_u = 8314.3 \text{ J kmol}^{-1} \text{ K}^{-1}$ $= 0.0821 \text{ L atm mol}^{-1} \text{ K}^{-1}$

List of Symbols

A	Cross-sectional area	m^2
A_{ht}	Heat transfer surface area	m^2
c	Effective exhaust velocity	m s^{-1}
c_w	Average coolant water specific heat	$\text{J kg}^{-1} \text{K}^{-1}$
c^*	Characteristic velocity	m s^{-1}
C_d	Discharge coefficient	1
C_F	Thrust coefficient	1
d_{gap}	Annular coolant water flow gap	m
D	Diameter	m
F_T	Thrust	N
I_{sp}	Specific impulse	s
k	Ratio of specific heats	1
L	Length	m
L^*	Characteristic chamber length	m
\dot{m}	Mass flow rate	kg s^{-1}
\mathfrak{M}	Molecular mass	g mol^{-1}
M	Mach number	1
p	Pressure	Pa or atm
q	Average heat transfer rate	W m^{-2}
Q	Rate of heat absorption	$\text{W} (\text{J s}^{-1})$
r	Propellant mixture ratio	1
R	WF gas constant	$\text{J kg}^{-1} \text{K}^{-1}$
S	Maximum allowable working stress	Pa
t	Wall thickness	m
$time_{test}$	Rocket engine test burn time	s
T	Temperature	K
v	Velocity	m s^{-1}
V	Volume	m^3
\dot{V}	Volume flow rate	$\text{m}^3 \text{s}^{-1}$
α	Nozzle divergence half-angle	°
β	Nozzle convergence half-angle	°
ϵ	Nozzle area ratio	1
ρ	Mass density	kg m^{-3}

Symbol subscripts:

a - ambient, **c** - combustion chamber, **con** - converging cone, **cw** - thrust chamber wall, **div** - diverging cone, **e** - nozzle exit, **f** - fuel, **inj** - injector, **jw** - cooling jacket wall, **l1** - location 1, **l2** - location 2, **o** - oxidiser, **op** - operating, **t** - nozzle throat, **tank** - propellant tank, **w** - coolant water, **1** - outer diameter of combustion chamber, **2** - inner diameter of cooling jacket

Chapter 1

Introduction

The science of propulsion is one that has been refined for millennia, and the rocket was invented based on the underlying fact that mass can be set in motion in one direction by expelling particles in the other. Propulsion can be achieved with various methods, each with its own advantages and disadvantages and most with a set of intrinsic hazards. That which all modern rocket propulsion systems have in common, however, is the need for system testing before mission operation.

To test not only each part of the system, but the operation and performance of the system as a whole, is essential. For the conducting of functional tests, complete propulsion systems are usually incorporated into a static structure - or test platform - where system processes can be remotely monitored and controlled. Rocket propulsion system testing is not only useful for industrial and commercial entities, but has an important role within academia as well. For many students and researchers it is important, from a learning perspective, to be able to apply theoretical knowledge in practice. For rocket engineering studies, this can be done by introducing into the curriculum, practical propulsion tests on a safe, uncomplicated and reliable test platform using theoretically predetermined parameter values. Such a platform would also offer the possibility for researchers to develop and test new propulsion technologies, e.g. additively manufactured thrust chambers.

1.1 Project motivation

Propulsion system testing facilities in Europe are few. Perhaps the most commonly used, and longest running, is the Lampoldshausen site in Germany - operated by the German aerospace center or Deutsches zentrum für Luft- und Raumfahrt (DLR) since 1962. Originally developed for liquid rocket engine testing, today the site is used for research within many areas related to propulsion systems. One of its main roles is to "plan, build and operate test beds for space propulsion systems on behalf of the European Space Agency (ESA) and in collaboration with the European space industry" [1]. Another example is the newly built engine test facility used by the Scottish rocket engine development company Skyrora, for their sub-orbital and orbital launchers [2]. These types of facilities are mainly or exclusively commercial, however, and there is a need for propulsion system testing platforms developed specifically for academic use. These types of platforms, to the knowledge of the author, do not exist in Europe at the time of writing.

Currently in Sweden, an increasing desire is being expressed by companies within the national space industry to develop their own propulsion systems and to initialise, or expand on, other propulsion related activities. For instance, Esrange Space Center (ESC) in the north of Sweden is currently expanding to facilitate more services. In operation since 1966, ESC provides services for the launching of sounding rockets and high altitude balloons for international research purposes, as well as satellite communication [3]. Recently, together with the Swedish government, the owner of ESC - Swedish Space Corporation (SSC) - has invested in a testbed, currently in development, to develop and test

propulsion technologies. These include "reusable launch technology for small and large rockets, more environmentally friendly engines, test flights, and satellite technology" [4]. SSC has also entered into collaboration with DLR in order to optimise the testing capabilities of both Lampoldshausen and ESC, developing "test facilities for micro launcher engine and stage tests" to "provide the infrastructure in Europe for the entire range of engine tests, including tests at an early stage of development, thus increasing the portfolio of testing opportunities in Europe" [5].

In order to meet these demands of the industry, the knowledge of and particularly the practical experience with propulsion systems and the testing of them must be increased within academia. Thus, pressure is put on universities to provide students and researchers with the necessary expertise, which is why a university owned and operated propulsion system testing platform would be useful. According to the project supervisor, Dr. Élcio Jeronimo de Oliveira, a similar project is ongoing in Brazil. There, the company Edge of Space is developing a test stand quite similar to the one presented in this report, on behalf of the Brazilian aeronautics institute of technology or Instituto Tecnológico de Aeronáutica (ITA). Fig. B.1 in Appendix B displays figures of a rocket engine combustion chamber developed by Edge of Space.

1.2 Objectives

The main objective of this master thesis is to develop a preliminary design of a complete rocket propulsion system testing platform, to be used primarily for academical purposes. The propulsion system will be of a small scale, it will use liquid propellants and create thrust through chemical combustion. It will be designed with three key words in mind: safety, simplicity and reliability. The work will include:

- Designing the system hardware, including the chamber where thrust is produced and the assembly for feeding the chamber with propellants.
- Designing the system software, consisting of a Digital Control and Instrumentation System (DCIS) with user interface.
- Testing the DCIS software using simulated parameters.

1.3 Project management plan

In any project, there is a need for planning, a project structure and resources to implement and manage the project according to the developed plan. In the case of this master thesis project, a standard document is used as a guide in order to aid in the managing process - namely the *Space project management - Project planning and implementation* standard from the European Cooperation for Space Standardization (ECSS) [6].

"ECSS is a cooperative effort of the European Space Agency, national space agencies and European industry associations for the purpose of developing and maintaining common standards" [6, p. 2]. The ECSS has developed many standards for use within the space activities in Europe, and [6] describes the management of larger scale space projects realised by organisations working in the space industry. It lists project planning and organisational requirements, describing what needs to be accomplished in order to complete a space project - including both ground and space segments - from the introductory mission analysis to the disposal of any launched products. The work to be done is divided amongst the project actors, according to an organisational structure, and into predefined project phases.

Considering the objective and scope of the project described in this report, it will in this case not be feasible to follow the standard exactly in all aspects. For instance, in order for the standard to be useful in as many projects as possible, it is aimed at the larger scale projects requiring a more detailed management plan. These projects take longer time and require extensive documentation at every step in the work process, as well as a large number of project actors with different areas of expertise. The project introduced in this report is of a smaller scale, however, and does not necessarily require the same level of comprehensiveness. As far as for the part of the project work to be done in this master thesis, the suggested organisational structure in the standard does not apply, as there is at this stage no multi-level customer-supplier chain consisting of multiple project actors or teams. Another difference is that this project does not have launch or space segments - as the rocket engine tests will be conducted on ground - and therefore these parts of the standard can be omitted.

With that said, many parts of the standard are relevant within this project. As such, the standard is - wherever applicable - used as a foundation for the management plan to be implemented in this thesis. The project at hand has been correlated with [6], where relevant and applicable tasks have been used as a guide for the development of the management plan shown below, listing a series of tasks to be accomplished.

- Perform an assessment of risks and safety concerns.
- Present system functions and technical and functional requirements.
- Weigh in risks and propose technical solution(s) for the system functions.
- Describe the hardware and software products part of the selected technical solution(s), which are needed to comply with the system functions.
- Estimate project costs.
- Present a preliminary system design.

Chapter 2

Literature Review - Propulsion and Control

This section presents an overview of propulsion systems and how they are tested and controlled. It is the belief of the author that all the referenced literature used in this review can be considered credible. For instance, perhaps the most referenced source material for this chapter is the 9th edition of Rocket Propulsion Elements, written by George P. Sutton and Oscar Biblarz. The book has been used for a long time, especially within academia, and "has been regarded as the single most authoritative sourcebook on rocket propulsion technology" [7]. As the authors of the book state:

Since its first edition in 1949 this book has been a most popular and authoritative work in rocket propulsion and has been acquired by at least 77,000 students and professionals in more than 35 countries. It has been used as a text in graduate and undergraduate courses at about 55 universities. It is the longest living aerospace book ever, having been in print continuously for 67 years. It is cited in two prestigious professional awards of the American Institute of Aeronautics and Astronautics. Earlier editions have been translated into Russian, Chinese, and Japanese. The authors have given lectures and three-day courses using this book as a text in colleges, companies and Government establishments. In one company all new engineers are given a copy of this book and asked to study it [8, p. xix].

Another document referenced greatly not only in this chapter but throughout the report as an integral part in the design development, is the manual entitled HOW to DESIGN, BUILD and TEST SMALL LIQUID-FUEL ROCKET ENGINES by Leroy Krzycki - described as a "classic text for experimental and "amateur" rocket scientists, engineers, and technicians" [9]. Since its first printing in 1967 it has been, and still is, a popular source of information for designing simple and safe rocket engines for anyone with limited experience in the field. It describes the complete process, from design concept to the manufacturing and safe testing of the finished product, in a very comprehensible manner making it an ideal source material for this application.

2.1 Propulsion systems

In order to place a payload in orbit around Earth - or send it further out into space - a rocket needs many different parts. Each part providing an important function which contributes to a successful mission. According to [10], in order to aid in the design of a rocket, these parts are usually divided into four main systems; The structural system, the payload system, the guidance system and the propulsion system. Arguably the most important of these is the propulsion system, the role of which is to produce enough force for the rocket to escape Earth's gravity in order to leave the surface, fly through the air and further into space.

Essentially, this feat is achieved by applying Newton's third law: *For every action there's an equal and opposite reaction*. By accelerating and expelling mass, or particles - also called the Working Fluid (WF) - out of the aft end of the rocket, a force is generated towards the ground which, in turn, produces a reaction force applied to the rocket in the opposite direction. This reaction force is what is called thrust and it is directed along the length of the rocket, towards the front end and going through its center of gravity [11], [12].

WF is, as such, the name for the collection of particles being accelerated and driven out of the rocket to create thrust. In its initial state, while stored in the system and at rest before launch, this particle collection is called propellant. Depending on the method being used for acceleration, the propellant either changes physical states or does not. In the latter case, the terms WF and propellant can be used interchangeably.

The supply of propellant in a rocket is critical - From [11, p. 31]: "The engine's ability to produce thrust will endure only so long as the supply of particles, or working fluid, holds out". The amount of propellant to be loaded in a propulsion system is therefore something that must be carefully calculated, to make sure the rocket can perform nominally until mission completion.

The efficiency of a propulsion system is partly dependent on the efficiency of the propellant used. This efficiency is measured by a parameter called specific impulse, or I_{sp} , and it can be described as "the ratio of the amount of thrust produced to the weight flow of the propellants" [12].

2.1.1 Types

Every propulsion system has three fundamental components: The propellant - or WF - for thrust generation, a way to accelerate the WF out of the rocket and, lastly, the nozzle, which is the rearmost part of the rocket from which the WF escapes after acceleration. The type of propellant used - and the method with which it is accelerated - is what defines the propulsion system type.

To propel a rocket, energy is needed - kinetic energy to be exact. The original source of this energy can be used to categorise the types of propulsion system. Modern rocket flight is conducted primarily within two general areas of propulsion, based on their energy source: Electric Propulsion (EP) and Chemical Propulsion (CP) [8].

Electric Propulsion

What sets EP apart from its counterpart is that the energy used to accelerate the WF is not sourced from the propellant but rather from solar energy conversion units and/or batteries in the form of electricity [8]. Sutton and Biblarz [8] and Berlin [13] state that EP can be divided into three main types: electrothermal, electrostatic and electromagnetic propulsion.

In *electrothermal propulsion*, the WF is a gas which is accelerated through a specially shaped nozzle (see Sec. 2.1.4) by thermodynamic expansion, caused by electric heating. The gas can be heated in two ways. In the first, current is led through one or more pieces of metal with high electrical resistance, making them dissipate heat which is then transferred to the WF as it passes by. Alternatively, heating can be achieved with the use of an electric arc, discharged directly through the gas. Most types of gases can be used as WF in this EP technology, however the best results have come from using the product gases caused by the catalytic decomposing of liquid hydrazine during operation [8].

The remaining two EP types do not utilise thermal expansion for the acceleration of the WF and therefore do not require a nozzle to produce thrust. In other words: "no enclosure area changes are essential for direct gas acceleration" [8, p. 638]. Instead, propulsion is achieved through the ionisation

of a neutral propellant - either a liquid, a solid or a gas - and the use of either an electrostatic or electromagnetic field [8], [13].

The WF in *electrostatic propulsion* consists of positive ions which are accelerated and directed by an electrostatic field, giving rise to thrust. The ions can be sourced from a liquid metal propellant - typically caesium - by letting a strong electrostatic field act on it. Alternatively, the ions can be produced by bombarding a neutral gas propellant - typically xenon - with electrons. Another method exists within this category in which the ions are replaced with microscopic droplets of a conducting liquid, usually non-metallic. This technology is however still under development [8], [13].

The last type, *electromagnetic propulsion*, utilises plasma as the WF. This neutral and conductive fluid is generated by heating a propellant with either an electric arc or electrical field. The propellant is often a gas - typically hydrogen or argon - but can also be a solid, most commonly teflon, where an electric arc is used to ablate and heat molecules from the propellant surface. When an electromagnetic field acts in a direction perpendicular to a current, which is led through the plasma, a Lorentz-force is generated which accelerates the plasma in a direction at right angles to both the current and the field [8], [13], [14].

Chemical Propulsion

In this area of propulsion the energy is found within the propellant itself and is converted to kinetic energy through chemical combustion. Just as in the case with electrothermal propulsion, the acceleration of the WF happens via thermodynamic expansion. Thus, for all CP, a nozzle with a changing internal area is required.

The operation of a CP system is relatively simple. In essence, two chemicals - a fuel and a source of oxygen, an oxidiser - are mixed together, becoming the propellant. The propellant is subsequently either decomposed using a catalyst or ignited within a combustion chamber using a source of heat, which starts a chemical reaction resulting in exhaust gas - the WF - and large amounts of heat. The heat causes the WF to expand into a nozzle where it is accelerated and finally ejected, resulting in thrust [12], [8].

Sutton and Biblarz state: "According to the physical state of the stored propellant, there are several different classes of chemical rocket propulsion devices" [8, p. 5]. The two main ones being solid and liquid CP, as suggested by [12].

Solid CP:

In a solid CP system, the propellant chemicals are mixed, moulded and cured in the combustion chamber before launch and then delivered to the rocket as a single unit. The solid propellant mixture is called the grain and it contains, in addition to a fuel and an oxidiser, a binder - acting as a glue to hold the other ingredients together - and various types of additives designed to improve the performance of the system in different ways [8].

Two main propellant types exists within solid CP, the Double-Base (DB) and the composite types. In the former, the grain is homogeneous and the oxidiser and fuel are blended within the major ingredient which typically is liquid nitroglycerine absorbed by a solid nitrocellulose. The composite solid CP system is the more commonly used type. It uses a heterogeneous grain with a crystalline oxidiser and a fuel powder, combined with a polymer binder. Usually the fuel and oxidiser in this type are aluminium and ammonium perchlorate, respectively [8].

The combustion process is started with an electrical igniter and from that point the process cannot be halted or controlled remotely in real time. Instead, the system will produce exhaust and thrust until the propellant has been consumed. However, certain design choices can be made at the time of

moulding which can give some control over the thrust generation during burning. The engine can be moulded with a hollow core, called perforation, in order to maximise the inside burning area and by extension the thrust. By changing the geometric shape of the perforation cross-section, the burning rate and mass flow are affected - in turn shaping the thrust profile over time [8], [13].

Liquid CP:

Liquid CP systems, as opposed to the solid variety, uses liquid propellant chemicals for thrust production. The mono-propellant type contains only a single liquid stored in one propellant tank. As with solid CP, the liquid can be homo- or heterogeneous, the latter a mixture of a liquid fuel and a liquid oxidiser. Mono-propellant systems do not require an igniter to create the WF, instead the combustion happens through catalytic decomposition of the propellant liquid [8]. Although this type of system is used today in some cases, the more common type is the bi-propellant system. From here on, whenever the term *liquid CP* is written by itself in the text, it should be assumed to be of the bi-propellant type.

In a bi-propellant liquid CP system, the propellant chemicals - a liquid fuel and a liquid or gaseous oxidiser - are stored in separate tanks. They are kept separated until they are injected into a combustion chamber where they are immediately blended together, becoming the propellant which is then ignited to create the combustion gases used as WF. The assembly of the propellant injector, the combustion chamber and the nozzle is often referred to as the **thrust chamber**. There can be more than one thrust chamber connected to a single propulsion system [11], [8].

In addition to the propellant chemical tanks and the thrust chamber(s), liquid CP systems contain another important component - the **propellant feed assembly**, or the feed mechanism. It is the role of this assembly to feed the fuel and oxidiser from their respective storage tanks to the thrust chamber in a controlled and safe manner. This can be done in one of two ways; either by expelling the liquid out of one end of the tank by connecting a supply of highly pressurised gas to the other, or by connecting turbine driven pumps to the tank outlets [8].

Regardless of the feed method being used, all propellant feed assemblies contain some other essential parts. Piping is needed to transfer the liquids under pressure and several precise valves of different types are used for the filling and draining of tanks, to start and stop system processes and to accurately control these processes by regulating mass flow rates and pressures at set locations within the assembly. To prevent debris from entering the valves - possibly causing malfunctions - filters are often placed at different locations inside the piping. Furthermore, in order to achieve the level of control needed in this type of propulsion system, sensors measuring parameters such as magnitudes of flow and pressure are also required [8].

2.1.2 System comparison

EP vs CP

The WF in EP is either a gas, plasma or a collection of ions, meaning the expelled mass is quite small. Also, the energy used to accelerate the WF is not contained within the propellants but is rather supplied by a combination of external power units - such as solar panels, batteries and power-conditioning units. These units are relatively inefficient, have relatively large mass and the technology can only achieve low levels of WF acceleration. Consequently, in relation to CP systems, the thrust levels of EP systems are very low - usually between 0 and 2 N. As such, utilising EP to launch rockets from high-gravity bodies such as the Earth is not possible due to the unrealistically massive power sources that would be needed to reach the required thrust levels. Launch vehicle operations are therefore limited to CP while EP technology is used for satellite operations in low-gravity and

gravity-free environments. Today, satellites contain a multitude of subsystems requiring electrical power. Therefore, the added mass of a specific EP power source can be avoided by sharing the source with other subsystems on-board. Due to the low thrust levels, EP operations take longer time to perform and are therefore usually of a non-urgent type, e.g. orbital station-keeping or momentum-dumping operations [8] [13].

On the other hand, the low propellant mass flow - or weight flow - of EP systems combined with their ability to produce very high exit velocities, results in high propulsion efficiency. Values of I_{sp} are in the order of thousands of seconds compared to hundreds of seconds for CP systems. Velocity changes take a long time to perform, due to the low accelerations, but a large amount of impulse can be achieved while consuming a small amount of propellant. This makes EP systems ideal to be used as the primary propulsion system on propellant-limited satellites for long-duration space missions. Another advantage with EP is that the storage and handling of hardware is relatively safe and uncomplicated, compared to CP where some propellants automatically combust when in contact with each other or in some cases have to be continuously kept at very low temperatures [8] [13].

Solid CP vs Liquid CP

Solid CP systems are relatively simple to operate compared to their liquid counterpart. They have very few moving parts, do not leak and are ready to be ignited instantly. After being moulded, a solid rocket engine requires little maintenance and can spend up to 30 years in storage before becoming unusable. Due to the high propellant density, and consequently relatively small size, these engines are often the preferred type for the so called "strap-on" propulsion stages, used to add to the thrust of the first stage - the boost stage - of launch rockets. Perhaps the largest drawbacks of solid CP are that the engines are generally non-reusable, generated thrust can not be varied during flight and the propulsion system can not be tested fully before a flight. Another disadvantage is that the propellant grains are generally very sensitive to mechanical stress or temperature changes - should a fissure develop in the grain, combustion could easily follow which could result in explosion. This places heavy demands on ground handling and storage environments, especially since the inseparability of casing and propellant entails that engines are always transferred fully loaded [8] [11].

Liquid CP systems are more complex since they have many moving mechanisms and precise instruments. Although these components - together with propellant tanks and feed lines - generally make this kind of system heavier than the solid counterpart, they also permit a more controlled operation. Thrust can be varied in-flight by remotely regulating the propellant transfer process and the system can also be shut off and restarted at will. Contrary to solid rocket engines, the propellant supply is separated from the thrust chamber which means that one supply can be used to feed several chambers. Also, ground handling is safer since the system can be transferred empty and filled with propellant just before a test or launch. Within this CP category, mono-propellant systems have the simplest design and require only one propellant tank. However, by using a catalyst for combustion, thrust generation is limited and the efficiency is relatively low. Comparatively, bi-propellant systems are generally more efficient and have higher values of I_{sp} than both mono-propellant systems and solid CP. This, together with repeatable and more controlled operation makes bi-propellant liquid CP systems in many cases ideal to use as primary propulsion systems in launch vehicle stages. As they are restartable and can provide highly accurate control, smaller liquid CP systems can be used to achieve precise movements by firing thrusters in short, repetitive pulses. This makes this system type uniquely suitable for most attitude operations on launch vehicles and satellites. One big disadvantage with liquid CP is that most propellant types are hazardous and any spills can be highly toxic or corrosive [8] [13] [11].

2.1.3 Bi-propellant liquid propulsion systems

Liquid propulsion systems are rather complicated when compared to the alternatives, e.g. solid CP. But with this complexity comes benefits, such as significantly increased thrust control and the option to stop and restart the combustion process. This section will further describe the bi-propellant liquid propulsion system and its constituents, as well as discuss options for its propellant chemicals.

Design

As mentioned earlier, the fuel and oxidiser are kept in separate storage tanks. In the case of gas pressure feed systems, at least one additional tank to store the gas is usually included as well. In many cases, these tanks take up a large part - if not a majority - of the space in a rocket [10]. Therefore, their location, as well as their mass, must be taken into consideration as they affect the location of the rocket's center of gravity [8].

As with any rocket part, mass must be kept to a minimum while still being able to handle large mechanical stress. To comply with these requirements, one must use the right material and according to Sutton and Biblarz, "Common tank materials are aluminum, stainless steel, titanium, alloy steels, and fiber-reinforced plastics" [8, p. 196]. Also according to [8], the optimal tank shape is a sphere, as it yields minimum mass for a given volume. However, this tank design is often not a viable option for larger tanks, as the shape does not efficiently fill up usable interior rocket space. For this reason, cylindrical tanks are more common.

In order to feed the propellant liquids from their respective tanks to the thrust chamber(s), one of two main techniques can be utilised. The first is to connect centrifugal pumps - driven by one or more turbines - in the piping downstream of the tanks, which deliver the liquids to the remaining propulsion system. The second propellant feed assembly technique is the so called gas pressure feed system. Here, instead of pulling the liquids out of the tanks with downstream pumps, they are pushed out using high pressure gas acting upstream of the liquids. Generally, the pressurising gas is either helium or nitrogen. Two types of feed system exist within this category. The first is the "blow-down" system where the gas is stored inside the fuel and oxidiser tanks. In this system the liquids are evacuated as the stored gas expands in the tanks, however the gas pressure is not regulated and will decrease over time. In contrast to the blow-down system, in the second and perhaps more commonly used type the gas is stored in one or more external tanks. The gas is then fed into the tanks with a special valve called a gas pressure regulator valve. This method results in a more controlled operation as the pressure regulator is able to keep the pressure - and consequently the thrust - at a near constant level [8].

Two fundamental parts of a liquid propulsion system are the pipes and the valves. The pipes, usually metal with welded joints, are used to move fluids between system components and the valves are used to control these movements. Other than gas pressure regulator valves, isolation and latch valves are used. The former to isolate sections of the system when closed and the latter for repeatedly closing off and opening sections during operation, using small amounts of electrical power for valve activation. So called check valves can be used to only allow fluid flow in a single direction [8].

Before entering the thrust chamber(s), the propellant liquids are usually filtered to prevent debris particles from entering and possibly creating small holes, causing failures. Filters can also be used at other locations in the system to protect valves from the debris [8].

When it comes to thrust generation, the ratio of oxidiser to fuel in the propellant is an important parameter. According to [8], this mixture ratio - r - is defined as "the ratio of the oxidizer mass flow rate \dot{m}_o to the fuel mass flow rate \dot{m}_f " [8, p. 194] and it affects the chemical properties of the WF.

The value of r is in most cases chosen so as to maximise the specific impulse of the system and it is directly determined by the propellant injector of the thrust chamber.

The propellant injector measures and divides the incoming streams of propellant liquids, after which they are sprayed into the combustion chamber. The oxidiser and fuel are blended and distributed uniformly across the injector face inside the chamber and then ignited. Many different injector designs exist and are chosen depending on the desired value of r or the desired efficiency and stability of combustion. Small spray nozzles are often used to directly inject the propellants as droplets in conic shapes. This method is usually the most effective at breaking up, mixing and evenly distributing the liquids into a propellant with the desired chemical properties [8], [15].

The burning of the propellant inside the combustion chamber releases extreme amounts of heat and results in very large internal pressure levels. The choices made in the design of this chamber - as well as the nozzle - are of upmost importance, as they determine the capability of a safe and controlled operation of the propulsion system. According to [8], temperatures in the combustion chamber greatly exceeds the melting point of common wall materials. For this reason, cooling the thrust chamber walls is a necessity (see Sec. 2.1.5). Furthermore, the thickness of the walls is another important design parameter as they must withstand the high pressure of the combustion gases - including temporary surges in pressure at propellant ignition.

The common combustion chamber shape is cylindrical, leading into the nozzle at one end and flat at the other where the propellant liquids are injected. The chamber volume must be large enough so that all injected propellant can be properly mixed and combust entirely before arriving at the nozzle. Increasing the volume also reduces pressure loss in the chamber - which has a negative impact on system performance. On the other hand, increasing the chamber size also increases the mass - which should be kept at a minimum. Thus, a compromise between weight and performance is required [8].

An example of a gas pressure fed liquid propulsion system with an external pressurising gas tank is shown in Fig. 2.1.

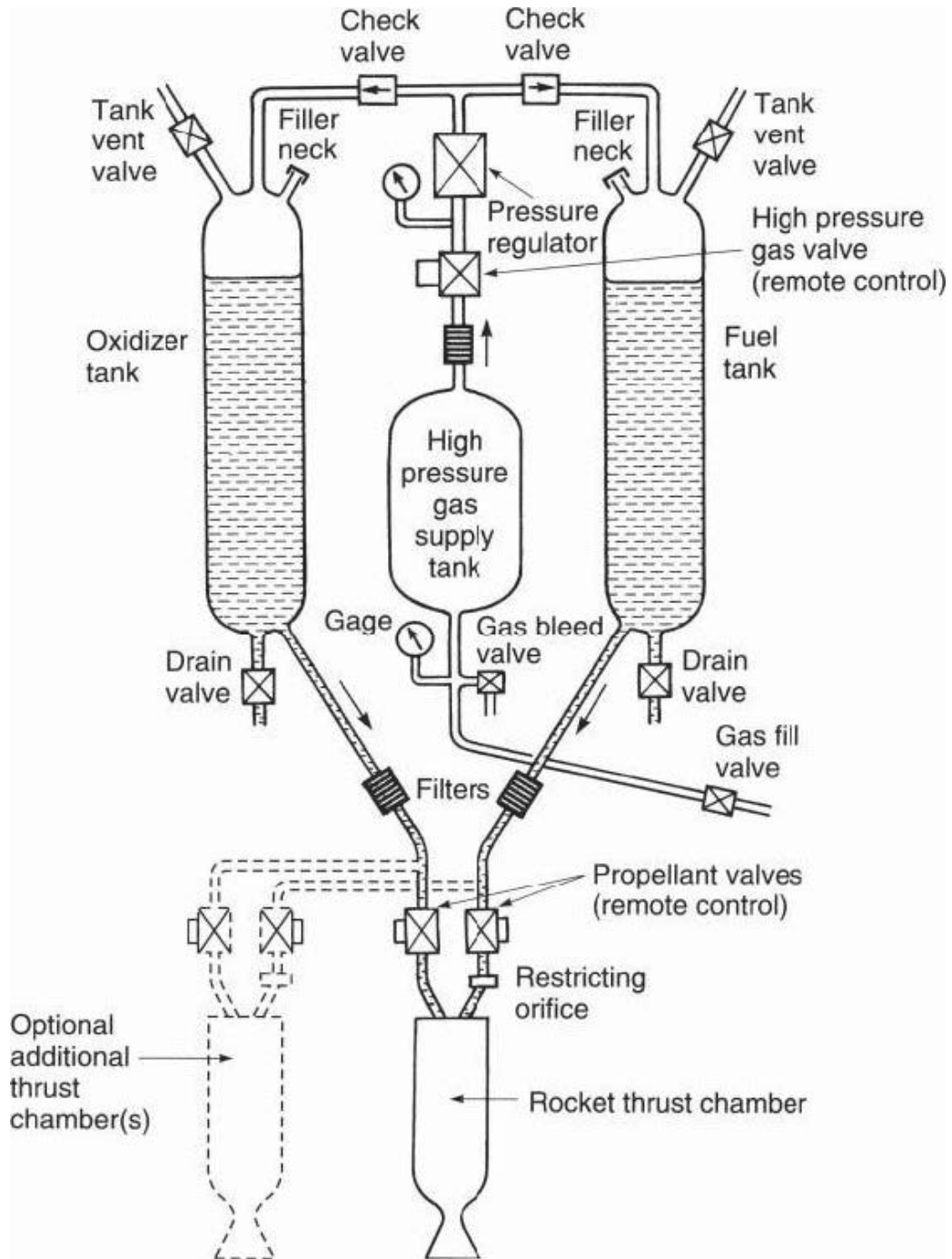


FIGURE 2.1: Example flow diagram of a bi-propellant liquid propulsion system fed by an externally stored pressurised gas. Included are all essential components in a liquid propulsion system, e.g. propellant liquid tanks, valves and thrust chamber(s) [8]. Image used in accordance with Section 107 of the 1976 United States Copyright Act.

Propellants

The choice of a propellant combination for a bi-propellant system is influenced by many factors. Physical properties, such as chemical stability and compatibility with hardware, should be considered. It should also be decided whether the liquids used should be able to ignite and combust

spontaneously at contact - i.e. hypergolic combustion - or if an external ignition source should be used. Generally, propellants are chosen based on their ability to generate thrust, i.e. their value of I_{sp} . Apart from this, what is important to consider are the many hazards that come with the handling and storing of chemical propellants for rocket propulsion [8]. Some common hazards, as listed in [8], are corrosion of containers and plumbing, fire and explosion hazards, propellant toxicity and other health hazards to the human body, such as skin burns. This section presents descriptions of some of the more common oxidisers and fuels and their intrinsic hazards.

Oxidisers:

One of the more widely used oxidisers, especially in larger rocket engines, is **Liquid O₂Xigen (LOX)**. It gives good performance and can be used together with a large variety of fuels, most commonly with hydrogen but also with hydrocarbon fuels such as gasoline, ethanol and kerosene. LOX is noncorrosive and nontoxic, however it is a cryogenic propellant meaning that it becomes liquefied at freezing temperatures. Therefore, if in contact with human skin, it can cause severe frostbite. Spontaneous ignition with organic materials is not common at ambient temperatures, however if mixed with them and put under pressure or induced stress combustion and detonations can occur. LOX "supports and accelerates the combustion of other materials" [8, p. 256] which means that any contact materials must be clean for safe storage and handling. Since it is cryogenic, it must be kept at low temperatures. Thus, it can not be readily stored for long and all parts of the propulsion system containing the propellant must be insulated to minimise evaporation. This complicates both handling and storage [8]. A less hazardous version of LOX, with less complicated handling and storage, is **Gaseous Oxygen (GOx)**. GOx is stored at ambient temperatures, meaning no special storage provisions are needed. It "can be readily and inexpensively obtained in pressurized cylinders in almost any community" [15, p. 7] and is relatively safe to handle [15].

Nitrogen TetrOxide (NTO) or dinitrogen tetroxide (N_2O_4) is "the most common storable oxidizer employed today" [8, p. 258] possibly because it can be "stored indefinitely in sealed containers made of compatible materials" [8, p. 258]. It is hypergolic with hydrazine and its derivatives - MonoMethyl-Hydrazine (MMH) and Unsymmetrical DiMethylHydrazine (UDMH) - and can induce spontaneous ignition with common materials such as grease or wood. NTO in its pure form is mildly corrosive but can create strong acids if water moisture is absorbed. The temperature range for its liquid phase is relatively narrow, meaning that special storage provisions need to be taken in order to avoid freezing or vaporisation. The decomposition of NTO results in highly toxic NO₂ fumes [8].

Nitric Acid (HNO₃) is corrosive to many materials. For concentrated HNO₃, few materials - including gold and certain types of stainless steel - are compatible with the propellant to use for containers and plumbing etc. It is hypergolic with various chemical compounds - including hydrazine and different types of amines - and reacts with gasoline, alcohols, hydrazine etc. Reactions with certain wall materials can cause the formation of nitrates which changes the oxidiser properties, possibly causing blockages within valves and plumbing. The most common type of HNO₃ is Red Fuming Nitric Acid (RFNA) which, compared to the concentrated variety, is more stable and less corrosive. On the other hand, evaporated RFNA fumes are very poisonous and HNO₃ droplets on skin "causes severe skin burns and tissue disintegration" [8, p. 251] [8].

Fuels:

Similarly to LOX, **Liquid Hydrogen** is a non-toxic, non-corrosive propellant. It is also cryogenic, meaning that many of the same hazards and storage complications that come with LOX usage are applicable for this propellant as well. In fact, liquid hydrogen is the coldest of the known fuels with a 20 K boiling point. It is also the fuel with the lowest density which makes large and bulky storage tanks a necessity. Apart from the requirement of well insulated propulsion system parts for evaporation minimisation, the thorough emptying of air and moisture from plumbing and tanks before propellant filling is very important. This is because "All common liquids and gases solidify

in liquid hydrogen. Such solid particles in turn plug orifices and valves" [8, p. 261]. There is also an explosion risk if liquid hydrogen is mixed with solidified air or oxygen particles. Furthermore, hydrogen gas, from which liquid hydrogen is made, is "highly flammable and explosive over a wide range of mixture ratios" [8, p. 262] when exposed to air and provisions for intentional ignition of excess gas is often a requirement [8].

Hydrazine (N_2H_4) is a toxic propellant with a relatively high freezing point. Because of this, electrical heating of system parts containing the propellant is usually implemented. On the other hand, apart from its pure form, thermally it is relatively unstable compared to other fuels. If it is heated too much it decomposes and in some cases this can lead to the release of energy in the form of explosions. For N_2H_4 vapours under pressure, decomposition can happen at lower temperatures than for the liquid type and the vapours can also ignite spontaneously when mixed with air. As mentioned previously, N_2H_4 is hypergolic with certain oxidisers such as NTO and HNO_3 and reacts with various materials including iron, copper and magnesium - possibly inducing decomposition. Ingestion of the propellant and inhalation of its vapours can be harmful and skin contact "may cause nausea and other adverse health effects" [8, p. 251]. N_2H_4 and its derivatives "are known animal and suspected human carcinogens" [8, p. 251]. In general, N_2H_4 , UDMH and MMH have similar properties. Thermally, **UDMH** is a slightly more stable liquid than N_2H_4 . **MMH** is more resistant to blast waves and suppresses explosive decomposition when certain amounts of it are mixed in with N_2H_4 [8].

Hydrocarbon fuels are chemicals consisting of hydrogen and carbon derived from naturally occurring compounds, namely petroleum and natural gas. Compared to most other types of fuel, hydrocarbon fuels have relatively low cost, high availability and generally simple handling and storage. For a given oxidiser, this fuel type is often less efficient at producing thrust than other types. On the other hand, hydrocarbon fuels generally have a higher density which allows for a more efficient utilisation of propellant supply tanks, due to a larger mass being provided for a given volume [8].

Petroleum-based fuels include different types of alcohol - e.g. ethyl alcohol, or **ethanol** - **gasoline** and **kerosene** - including specially refined kerosene fuels such as **jet fuel** and **Rocket Propellant (RP)-1** and **RP-2** [8]. The fuels and their vapours are highly flammable, although non-hypergolic [16] [17] [18]. They are non-corrosive [17] [19] [20], normally chemically stable - meaning they are not normally self reacting - and can be stored at ambient temperatures with no special provisions other than good ventilation [16] [17] [18]. If not properly ventilated however, the combustion products of these fuels (e.g. CO_2) can reach dangerous levels "which may cause unconsciousness, suffocation and death" [16, p. 8]. Strong acids, e.g. Nitric acids, and other oxidising chemicals should be avoided [16] [17] [18]; contact with ethanol will cause violent reactions and possibly explosions and for the remaining fuels incompatibility is suspected [21] [22] [23] [24]. Regarding health hazards and toxicity, the fuels are confirmed to be carcinogenic for animals but whether they are for humans is unknown. Skin contact causes mild to moderate irritation for all fuel types and eye exposure causes mild irritation with kerosene, moderate with gasoline and serious with ethanol and jet fuel. With the kerosene type fuels and gasoline, inhalation of fuel vapours causes moderate irritation of the respiratory system and with ethanol it has intoxicating effects. Mild to moderate dizziness might also occur. Prolonged exposure to ethanol and gasoline can cause more severe damage, such as skin inflammation and other organ damage [16] [17] [18] [25].

Sourced from natural gas, **Liquid Methane (CH_4)** is a relatively common hydrocarbon fuel. Compared to the petroleum derived fuels, liquid CH_4 is the most hazardous in terms of flammability and health according to the National Fire Protection Association (NFPA) [26] [21] [22] [23]. It is extremely flammable and will explode if mixed with strong oxidisers, however chemically it is normally stable [26]. Other incompatible chemicals are fluorinated and halogenated compounds [27]. It is non-corrosive to most common plastics and metals, including stainless and carbon steel, brass, copper and aluminium alloys [28] [29]. The fuel is cryogenic [8], entailing more complicated storage than for other hydrocarbon fuels. Also, direct skin contact with the fuel can cause frostbite and eye

exposure can result in blindness. Vapour inhalation is not considered to be toxic however inhaling large quantities is asphyxiating. Skin or eye contact with the vapours is harmless. CH₄ does not cause cancer in humans [27] [28].

2.1.4 Nozzle design

The magnitude of the thrust produced in a rocket is determined by the amount of WF mass that flows through the nozzle each second - the mass flow rate - and the WF exit pressure and velocity at the nozzle exit. The mass flow rate is partly determined by the cross-sectional area of the nozzle. Moreover, the area ratio - from the smallest cross-sectional area, the throat, to the exit area - determines both the pressure and velocity of the WF at the exit [30]. Thus, the way the nozzle is designed directly determines the amount of thrust that can be produced for a given WF, making the nozzle an important element in the determination of a propulsion system's performance.

It can be shown that a maximum mass flow rate through the system can be achieved if the flow is choked at the throat. This happens when the throat area is decreased until the speed of the mass flow at the throat is equal to the speed of sound, i.e. the Mach number (M) of the flow is equal to one [31]. It can also be shown that if the flow is choked at the throat and the cross-sectional area downstream of the throat is continuously increased, the velocity of the mass flow will become larger than the speed of sound and reach a maximum at the nozzle exit [32].

Of course, when it comes to increasing thrust, maximising both the exit velocity and the WF mass flow rate is desired. Most rocket nozzles used today are hence designed with a fixed convergent section leading into a throat, followed by a fixed divergent section leading to the nozzle exit. This type of nozzle is called a Converging-Diverging (CD) nozzle [32] or a de Laval nozzle [15]. It is the most efficient nozzle type attainable in terms of utilising a given WF for maximum thrust yield. A version of this nozzle type can be seen in Fig. 2.2.

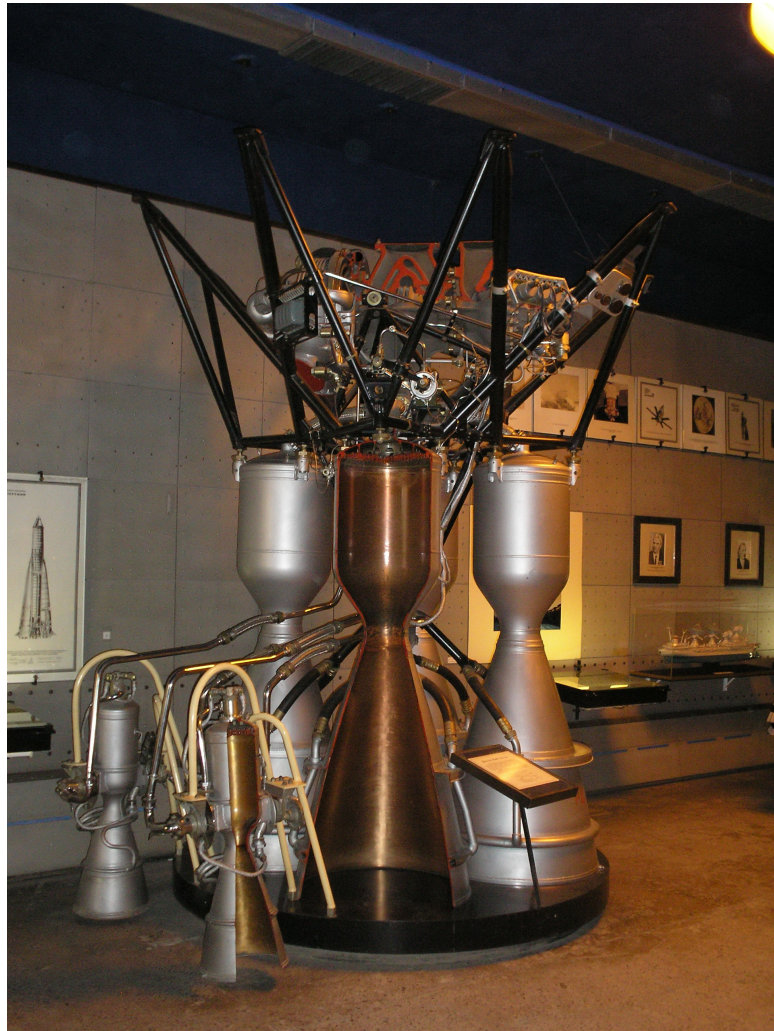


FIGURE 2.2: The Converging-Diverging rocket nozzle design, also known as the de Laval nozzle. Seen here in cross-section together with the combustion chamber as part of the Russian RD-107 rocket engine. Image source: https://commons.wikimedia.org/wiki/File:RD-107_Vostok.jpg (Accessed 19/05/24). Photograph by A. Sdobnikov, 2008, The Museum of Space Exploration and Rocket Technology, St. Petersburg Russia.

Image use permitted under the Creative Commons 3.0 license.

2.1.5 Thrust chamber cooling

Chemical combustion results in exhaust gas and substantial amounts of heat. The heat is absorbed by the gas, reaching temperatures as high as 4100 °C, after which a portion of the heat is transferred at high rates to the inner surfaces of the combustion chamber and nozzle - almost exclusively through convection. If left unregulated, the absorbed heat will continuously decrease the chamber wall strength - as well as increase wall erosion due to increased chemical oxidisation - eventually causing the inner wall to fail and break apart from the induced loads. Therefore, the implementation of thrust chamber cooling provisions is crucial for sustainable propulsion system use. The criticality of adequate cooling increases with decreasing thrust chamber size [8].

Based on how the heat is transferred there are two commonly used cooling methods. For unsteady heat transfer - where temperatures do not stop increasing during the combustion process - the **transient cooling** method is used. With this method, the maximum combustion duration is determined

by how well the thrust chamber enclosure absorbs heat and "Rocket combustion operation has to be stopped just before any exposed walls reach the critical temperature at which it would fail" [8, p. 290]. This type of cooling can be done by making the chamber walls completely out of metal and "sufficiently thick to absorb the required heat energy" [8, p. 291], however this only allows for a combustion duration in the order of a few seconds. A longer duration can be achieved with another transient cooling type - **ablative cooling**. Here, the inner chamber surfaces are coated with a layer consisting of hard fibres coated with an organic binder. When exposed to heat the binder decomposes and forms a cooling gas layer on the wall surfaces [8].

Steady-state heat transfer cooling is the second method. In this method, heat is continuously led away from the enclosure, making the temperature of the walls reach a steady state during combustion. With **radiation cooling** this can be done by radiating the heat directly from the outer surface of the chamber to empty space, by making the wall out of a heat radiating high-temperature material, e.g. rhenium. Probably the most common steady-state cooling technique, and the most widely used today, is **regenerative cooling**. In this technique, one of the propellants is used to absorb the transferred combustion heat by letting it circulate, either through cooling channels milled into the chamber wall or through a passage concentric to the outer wall and encased by a cooling jacket, before being fed through the injector and burned. The heat absorption leads to a small, but measurable, energy increase in the propellant which in turn slightly increases its performance [8].

Another method similar to regenerative cooling is **water cooling**. Here, the coolant liquid is an external supply of water instead of one of the propellants. One disadvantage with this cooling method is that the released energy is not collected and used for the combustion and so the added performance received with regenerative cooling - albeit minor - is lost. On the other hand, with regenerative cooling - if using a hydrocarbon fuel - carbon deposits can be formed inside the cooling channels which impedes the heat transfer [8], something which is avoided with a water coolant. Water cooling was used for rocket engines during the 20th century and was a popular method used by rocket pioneer Robert H. Goddard [33], however in modern times is not commonly used for flight engines - possibly because of the inefficiency that comes with the added mass of an external water supply on-board the rocket. For static rocket engine testing, however, it is a viable option [15] and has been used in recent designs for testing purposes [34].

Materials used for the thrust chamber walls need to have good heat conduction while being able to withstand high mechanical stress and erosion due to oxidisation. Many materials fit this description to various degrees, however many are advanced, expensive and not readily available. One commonly used low-cost material is copper, which has good conductive properties and oxidisation resistance [8] [15]. For cooling jackets, stainless steel or brass is recommended [15].

2.2 Propulsion system testing

The propulsion system of a rocket is always subjected to various tests before being used in an actual mission. These include factory tests such as inspections of specific parts or functional tests of components. Tests are usually performed on the system where certain aspects of the mission environment is approximated closely, such as vacuum chamber and shake tests, to confirm that the system will work under planned conditions. Often, however, a complete propulsion system is tested outside mission conditions to evaluate general functionality and performance. Here, the complete assembly is mounted to a static test stand on ground [15]. In some cases a system is developed to be used solely for on-ground static testing, in which case usual mission limitations on for example weight and size do not necessarily apply. The system of which the design is to be developed in this thesis is an example of such a system.

The testing of propulsion systems is dangerous, especially when working with highly flammable propellants designed to combust at high pressures and temperatures. Thus, when developing the physical design of a static test stand, the safety of the operator must always be considered and various safety provisions must be implemented.

Engine explosions, and the ejected shrapnel following them, represent the most hazardous possible outcome of rocket engine testing and protection measures should be implemented against them. Suitable barriers should be placed in every direction around the test stand. The operation of the system must happen remotely, from an operator station located at a distance of at least 6 m (20 ft) from the stand, behind one of the barricades. A steel framework structure should be used for component mounting, for increased rigidity. It is also recommended to physically separate the engine - or thrust chamber, the fuel tank and the gas supplies from each other with barricades in-between, in order to reduce the potential damage should an explosion occur [15].

2.3 Digital Control and Instrumentation System

Depending on the type of propulsion system implemented, the level of required system control varies. In the case of a liquid propulsion system, the control of components such as valves and regulators - as well as the measurements of critical parameters - is essential for a safe and precise operation. Due to the inherent hazards of rocket engine propellants, the remote operation of such systems is absolutely necessary to ensure the safety of the operator. Remote operation has become simpler with the introduction of digital and electrical control and measurement components. A half-century ago, remote propellant flow regulation would be done by manually operating control valves using valve stem extensions made of pipe and pressure was commonly only measured with analog gauges. Electrical sensors existed, however they were quite expensive compared to today [15]. In modern propulsion systems on the other hand, solenoid valves and pressure transducers sending signals through wire or wirelessly to the operator station are often used instead. An example case is a recent rocket engine test stand design [34].

The hardware is only a part of the system however. Equally important is the software that controls it and reads and displays measured parameter values to the user - the DCIS. Many programs can be used for the design of such a software. An example is the .NET Framework from Microsoft, which can be used to develop various custom applications using traditional programming languages such as C# [35]. Recently, this software product was used to design the user interface for the DCIS used for the test platform designed as part of ThrustMe's TESl Platform for Electronics Modules in Electric Thrusters (TESPEMET) project [36]. Another program that can be used for DCIS development, using another type of programming language, is LabVIEW. This program is planned to be used for the software design in the project presented in this thesis.

LabVIEW is a program developed by National Instruments, originally as "a tool for scientists and engineers to facilitate automated measurements" [37]. It uses a graphical programming environment which provides visual representations of actual system components, along with tools for creating easily interpreted custom user interfaces. The program also provides the possibility to integrate with virtually any hardware through software interfaces called drivers, developed and ready to use for many instruments and devices. This means that LabVIEW can be used to design a multitude of different types of system with various applications - for control, measurement or testing - and today it has become a standard within many engineering industries [37] [38].

Chapter 3

Theoretical Background

3.1 Design equations

This section presents all underlying equations used in the development of the preliminary test platform hardware design. For this design, with the aim of simplifying the calculation process, the rocket propulsion system described is assumed to be ideal. Valid assumptions in the ideal case, concerning thrust chamber processes, are listed in [8]. For example, the WF is assumed to comply with the ideal gas law and to have a homogeneous composition as well as being entirely gaseous. Furthermore, the gas expansion through the thrust chamber is considered to be isentropic, meaning heat and pressure losses are small and the generation of kinetic energy from chemical combustion is at a maximum. All equations presented here have been sourced from [8] and [15], unless otherwise stated.

3.1.1 Thrust chamber

Thrust and velocities

The total thrust in N generated in the thrust chamber is given by

$$F_T = \dot{m}v_e + (p_e - p_a)A_e, \quad (3.1)$$

where \dot{m} is the total propellant mass flow rate in $kg\ s^{-1}$, v is the average WF velocity in $m\ s^{-1}$, p is pressure in Pa and A is cross-sectional area in m^2 , the subscripts e and a representing nozzle exit and ambient properties respectively. The ambient pressure can - according to [39] - be calculated as

$$p_a = 101325(1 - 2.25577 \cdot 10^{-5} \cdot h)^{5.25588}, \quad (3.2)$$

where h is the altitude above sea level in m .

The average nozzle exit WF velocity can be described as

$$v_e = \sqrt{2RT_c \left(\frac{k}{k-1} \right) \left(1 - \left(\frac{p_e}{p_c} \right)^{\left(\frac{k-1}{k} \right)} \right)}, \quad (3.3)$$

where T is temperature in K , the subscript c representing combustion chamber properties, and k represents the ratio of specific heats of the WF. R is the WF gas constant in $J\ kg^{-1}\ K^{-1}$ given by

$$R = \frac{R_u}{\mathfrak{M}_{WF}}, \quad (3.4)$$

where R_u is the universal gas constant equal to $8314.3 \text{ J kmol}^{-1} \text{ K}^{-1}$ and \mathfrak{M}_{WF} is the molecular mass of the WF in g mol^{-1} .

The effective exhaust velocity is the "average or mass-equivalent velocity at which propellant is being ejected from the rocket vehicle" [8, p. 28] in m s^{-1} and can be written as

$$c = \frac{F_T}{\dot{m}} = I_{sp} g_0 = c^* C_F, \quad (3.5)$$

where g_0 is the average acceleration of gravity at sea level equal to 9.81 m s^{-2} , c^* is the characteristic velocity - an efficiency parameter of the engine - in m s^{-1} and C_F is the thrust coefficient.

Propellant mass flow rates

The following relations between the total propellant, the oxidiser and the fuel mass flow rates hold true:

$$\dot{m} = \dot{m}_o + \dot{m}_f \quad (3.6)$$

and

$$\dot{m}_f = \frac{\dot{m}}{r+1}, \quad (3.7)$$

where r is the propellant mixture ratio given by

$$r = \frac{\dot{m}_o}{\dot{m}_f} \quad (3.8)$$

and the subscripts o and f describe the oxidiser and fuel mass flow rates respectively.

Thrust chamber size

The nozzle throat cross-sectional area can be written as

$$A_t = \frac{F_T}{p_c C_F}. \quad (3.9)$$

The nozzle area ratio is given by

$$\epsilon = \frac{A_e}{A_t} = \frac{1}{M_e} \sqrt{\left(\frac{1 + \frac{k-1}{2} M_e^2}{1 + \frac{k-1}{2}} \right)^{\left(\frac{k+1}{k-1} \right)}}, \quad (3.10)$$

where M_e is the Mach number - the ratio between local velocity and the speed of sound - at the nozzle exit, given by

$$M_e = \sqrt{\frac{2}{k-1} \left(\left(\frac{p_c}{p_a} \right)^{\left(\frac{k-1}{k} \right)} - 1 \right)}. \quad (3.11)$$

The nozzle throat and exit diameters D in m can be expressed in terms of their respective cross-sectional areas with

$$D = \sqrt{\frac{4A}{\pi}}. \quad (3.12)$$

The characteristic chamber length of the combustion chamber - "the length that a chamber of the same volume would have if it were a straight tube whose diameter is the nozzle throat diameter" [8, p. 287] - in m is defined as

$$L^* = \frac{V_c}{A_t}, \quad (3.13)$$

where V_c is the combustion chamber volume - "the volume from injector face up to nozzle throat section so as to include the cylindrical chamber and the converging cone frustum of the nozzle" [8, p. 285] - in m^3 . This is given by

$$V_c = A_c \left(L_c + L_{con} \left(1 + \sqrt{\frac{A_t}{A_c}} + \frac{A_t}{A_c} \right) \right), \quad (3.14)$$

where L_c is the length of the combustion chamber up to the converging part of the nozzle in m and L_{con} is the length from the converging cone entrance to the nozzle throat in m . The latter can be approximated as

$$L_{con} = \frac{D_c - D_t}{2 \tan(\beta)}, \quad (3.15)$$

where β is the nozzle convergence half-angle in $^\circ$. Similarly, the length of the diverging cone, from the nozzle throat to the exit, in m can be approximated as

$$L_{div} = \frac{D_e - D_t}{2 \tan(\alpha)}, \quad (3.16)$$

where α is the nozzle divergence half-angle in $^\circ$.

The minimum thickness of the thrust chamber wall in m is given by

$$t_{cw, min} = \frac{p_c D_c}{2 S_{cw}}, \quad (3.17)$$

where S_{cw} is the maximum allowable working stress, in Pa , of the chosen material for the thrust chamber wall.

The cross-sectional injection area, in m^2 , for a simple circular orifice oxidiser injector is given by

$$A_o = \frac{\dot{m}_o}{C_d \sqrt{2\rho_{o, inj} \Delta p}}, \quad (3.18)$$

where C_d is a discharge coefficient, $\rho_{o, inj}$ is the oxidiser mass density in $kg\ m^{-3}$ at the injector entrance and Δp is the pressure drop across the injector in Pa . The mass density at the injector entrance can be written as

$$\rho_{o, inj} = \rho_{o, a} \left(\frac{p_{inj}}{p_a} \right) \left(\frac{T_a}{T_{inj}} \right), \quad (3.19)$$

where $\rho_{o, a}$ is the oxidiser mass density at the ambient pressure and temperature and the subscript inj represents oxidiser properties at the injector. According to [40], based on the ideal gas law, $\rho_{o, a}$ can be determined with

$$\rho_{o, a} = \frac{\mathfrak{M}_o p_a}{R_u T_a}, \quad (3.20)$$

where \mathfrak{M}_o is the molecular mass of the oxidiser in $g\ mol^{-1}$, p_a is the ambient pressure in atm and R_u is the universal gas constant, here as $0.0821\ Latm\ mol^{-1}\ K^{-1}$.

Chamber cooling

The annular coolant water flow gap - between the outer wall of the thrust chamber and the inner wall of the cooling jacket - in m can be written as

$$d_{gap} = \frac{D_2 - D_1}{2}, \quad (3.21)$$

Where D_2 is the inner diameter of the cooling jacket and D_1 is the outer diameter of the combustion chamber. The former can be written as

$$D_2 = \sqrt{\left(\frac{4\dot{m}_w}{\pi v_w \rho_w} \right) + D_1^2}, \quad (3.22)$$

where \dot{m}_w , v_w and ρ_w are the coolant water mass flow rate, flow velocity and mass density respectively and

$$D_1 = D_c + 2t_{cw}, \quad (3.23)$$

where t_{cw} is the actual thickness of the thrust chamber wall in m .

The coolant water rate of heat absorption in W is given by

$$Q_w = q_{cw} A_{ht} = \dot{m}_w c_w \Delta T_w, \quad (3.24)$$

where q_{cw} is the average heat transfer rate of the thrust chamber wall in $W m^{-2}$, c_w is the average specific heat in $J kg^{-1} K^{-1}$ and ΔT_w the desired temperature rise in K of the coolant water. A_{ht} is the heat transfer area in m^2 , in this case the outer surface area of the thrust chamber, given by

$$A_{ht} = 1.1\pi(D_c + 2t_{cw})L_c, \quad (3.25)$$

where the surface area of the nozzle is approximated to 10% of the combustion chamber surface area, as suggested by [15].

The minimum thickness of the cooling jacket wall is calculated in the same way as for the thrust chamber wall, however in this case with its own value of S giving

$$t_{jw, min} = \frac{p_c D_c}{2S_{jw}}. \quad (3.26)$$

3.1.2 Propellant feed assembly

Pressurised tanks

The required volume of a propellant tank is given by

$$V_{tank} = \dot{V} \cdot time_{test}, \quad (3.27)$$

where \dot{V} is the propellant volume flow rate in $m^3 s^{-1}$ and $time_{test}$ is the desired time for one complete rocket test burn in s .

From the method in [40], the GOx density inside the oxidiser tank is given by

$$\rho_{o, tank} = \frac{\mathfrak{M}_o p_{o, tank}}{R_u T_{o, tank}}, \quad (3.28)$$

where $p_{o, tank}$ and $T_{o, tank}$ are the pressure in atm and temperature inside the oxidiser tank, respectively, and $R_u = 0.0821 L atm mol^{-1} K^{-1}$.

According to Boyle's law, for an ideal gas with a constant temperature within a closed system the product of the gas pressure and the occupied volume remains constant in all system locations. In other words, for two arbitrary system locations - $l1$ and $l2$ - the following applies:

$$p_{l1} V_{l1} = p_{l2} V_{l2}. \quad (3.29)$$

Chapter 4

Hardware Design

This chapter describes the process of developing the preliminary design of the propulsion system hardware. MATLAB was used for all calculations as well as for plotting graphs used to determine certain parameter values. The MATLAB code is not included in the report but can be provided by the author if requested.

Parameter values were primarily calculated, using equations mainly from [8] and [15]. However, some design decisions are not based on calculations but rather rely on practical testing results or experience in the field. As such, in some cases parameters were given suggested values directly from [15]. Values were, whenever applicable, converted from imperial to SI units. In these cases, and whenever any other converted values are used, the original value given in the source is written in parentheses in the text directly after the converted value.

4.1 Requirements

4.1.1 Reasoning

Engine type

For the type of propulsion system to be developed, CP was chosen instead of EP. One of the reasons for this is that one of the long term objectives with the testing platform to be designed is to develop a rocket engine that could be used to propel an upper stage within small sized multi-stage launch vehicles. From Sec. 2.1.2, it is clear that this type of engine needs to be of CP technology. Also, EP rocket engines tend to be quite complex in their design and the goal of this thesis is to design a simple testing platform that can be used by most people.

As discussed, solid CP systems are much less complex than the liquid variety. However, safe storage and handling of propellants is essential for this application, making the sensitive propellant grain of solid rockets a nonviable option in this case. Furthermore, the testing platform will be used for repeatable rocket engine testing where multiple parameter values are to be collected and compared to calculated counterparts. It is therefore imperative to have a restartable and modular system that allows for precise control of several parameters simultaneously and where different components can be replaced and system sections modified, to allow for further design developments in the future. Thus, the only option is a liquid CP system. A bi-propellant system will be designed as opposed to a mono-propellant, in order to allow for larger amounts of thrust to be generated.

The decision to develop a smaller scale propulsion system - with a thrust level approximately in the order of hundreds of N - was taken early in the design discussions. Because the goal is to develop a simple and safe system, it was decided to avoid the added complexity, the increased risks and

possible complications that comes with larger engine sizes and propellant volumes. Thus, three values of desired thrust were initially considered; 100, 500 and 1000 N.

Propellants

The goal when selecting the propellants was to choose a combination which is as safe as possible, with the least complex storage and handling. Of course, the maximisation of performance is always desirable, however as can be seen in Sec. 2.1.3, the propellants giving the best performance are often the most hazardous and require the most amount of storage provisions. The personnel utilising the finished test platform, i.e. researchers and students, will be relatively untrained in propellant handling. Furthermore, for various reasons, the more hazardous a propellant is, the more expensive the usage of it is and the budget for this project will be limited. Thus, a compromise between performance and safety was made and the selected propellant combination is GOx together with a petroleum-based hydrocarbon fuel - as suggested in [15].

After discussing with the supervisor, ethanol was decided to be used as the fuel, or more specifically an ethanol-water mixture. This fuel type, together with gasoline, arguably has the highest availability of the analysed hydrocarbon fuels and is non-expensive, in addition to being relatively safe to handle. It has also been used in several Brazilian rocket engine design undertakings before [34] [41].

Thrust chamber and cooling

When it comes to the nozzle, in order to maximise performance and WF efficiency a de Laval nozzle will be used for the design.

Cooling of the thrust chamber is a necessity, as described in Sec. 2.1.5. Transient cooling methods are not an option, since the combustion duration of the thick metal wall method is too short for the type of testing that will be performed with the platform and ablative cooling requires a too complex design. Instead, steady-state cooling will be used, specifically water cooling - as it is safe, simple and has been used in similar applications before [34]. As recommended in [15], the chamber will be covered by a concentric cooling jacket of the same shape as the chamber with the water coolant flowing in-between the layers.

Readily available and relatively low-cost materials will be used for the purposes of this design. By recommendation [15], copper is the chosen material for the thrust chamber and stainless steel will be used for the cooling jacket. As stated previously, copper is a good heat conductor. Stainless steel has quite high strength but also good corrosion resistance properties. Specifically, the chosen steel type is austenitic stainless steel of type SAE 316L which is a commonly used type with high temperature resistance and superior corrosion resistance compared to other types [42].

4.1.2 List of requirements

- Liquid bi-propellant CP system.
- Thrust level in the order of hundreds of N; 100, 500 or 1000 N.
- Oxidiser: GOx.
- Fuel: Ethanol-water mixture.
- de Laval thrust chamber nozzle type.

- Water cooling with cooling jacket.
- Copper for thrust chamber.
- Austenitic stainless steel type SAE 316L for cooling jacket.

4.2 Thrust chamber

The propellant combination chosen for this project is GOx as oxidiser together with a mixed solution of water and ethanol as fuel. Research has been made [43] to determine propellant parameters using this propellant combination. This research presents results of combustion simulations for varying concentration levels of ethanol in the fuel, corroborated with experimental trials. The results established the initial parameter values which were used as a base for the calculations presented in this section.

4.2.1 Nozzle sizing

The first step in the thrust chamber design was to determine the cross-sectional areas of the nozzle throat and exit, in order to get an initial idea of the chamber size. Eq. 3.9 was used to determine the throat area, using the three considered values of desired thrust in place of F_T . The value for the combustion chamber pressure p_c was assumed to be the same as for the thrust chamber used in the experimental trials described in [43], namely $p_c = 1.5 \cdot 10^6$ Pa. In addition, values of r , I_{sp} , T_c and c^* were also extracted from the information presented in [43], chosen for the maximum system performance cases - in terms of the highest resulting I_{sp} - as shown by the simulations. Three cases of Ethanol Fuel Concentration (EFC) - 70, 85 and 99.5 % - were considered and the extracted parameter values from each case are shown in Tab. 4.1.

TABLE 4.1: Values of four thrust chamber parameters for three cases of EFC. All values are taken from [43].

	EFC [%]		
	70	85	99.5
I_{sp} [s]	228	235	226
r	1.3	1.45	1.6
c^* [m s^{-1}]	1645	1675	1710
T_c [K]	3030	3120	3200

By rewriting Eq. 3.5, C_F can be written in terms of I_{sp} and c^* . Using the values from the case of EFC = 70 % in Tab. 4.1 gives $C_F = 1.359\dots$ and inserting this in Eq. 3.9, with $p_c = 1.5 \cdot 10^6$ Pa and for $F_T = 100$ N, gives $A_t = 4.903\dots \cdot 10^{-5} \text{ m}^2$.

To find A_e , the nozzle area ratio in Eq. 3.10 was first calculated and then multiplied with the value of A_t . In order to calculate ϵ , the value of k needed to be determined first. The WF produced in this rocket engine consists of a mixture of gases and therefore values of the gas specific parameters k and M_{WF} - of a WF resulting from using a certain EFC - were not initially known. To find these values, the following method was implemented:

Eq. 3.3 was combined with Eq. 3.4 and then rewritten into a new equation,

$$\frac{v_e^2}{2R_u T_c} = \left(\frac{1}{\mathfrak{M}_{WF}} \right) \left(\frac{k}{k-1} \right) \left(1 - \left(\frac{p_e}{p_c} \right)^{\left(\frac{k-1}{k} \right)} \right), \quad (4.1)$$

where the right-hand side is expressed in terms of the unknown parameters k and \mathfrak{M}_{WF} . Assuming optimum expansion of the WF, $p_e = p_a$. The testing platform is planned to be operated in Kiruna, Sweden and the average altitude over the sea at this location is 579 m. Inserting this as h in Eq. 3.2, with the optimum expansion assumption, gives $p_e = p_a = 9.455\dots \cdot 10^4$ Pa. Solving Eq. 3.1 for v_e with $p_e = p_a$, and comparing with Eq. 3.5, shows that $v_e = c$ for optimum expansion. The nozzle exit velocity can then be calculated in terms of the I_{sp} , according to Eq. 3.5, and for $EFC = 70\%$ $v_e = 2.236\dots \cdot 10^3$ m s $^{-1}$. This value, together with $T_c = 3030$ K, for $EFC = 70\%$ and $R_u = 8314.3$ J kmol $^{-1}$ K $^{-1}$, in the left-hand side expression of Eq. 4.1 gives a value of approximately 0.0993.

Next, the right-hand side expression was plotted in MATLAB - several times for different values of \mathfrak{M}_{WF} - against a range of k values, with $p_e = 9.455\dots \cdot 10^4$ Pa and $p_c = 1.5 \cdot 10^6$ Pa. The value ranges were chosen so as to find more precise values close to the approximate ones listed in [15] for the chosen propellant combination type, namely $k = 1.2$ and $\mathfrak{M}_{WF} = 24$ g mol $^{-1}$. By analysing the plots and finding a solution where the y-axis value is approximately equal to the calculated value of 0.0993, the value of k could be approximated. The generated MATLAB plots are shown in Fig. 4.1 with the selected k value curve point marked.

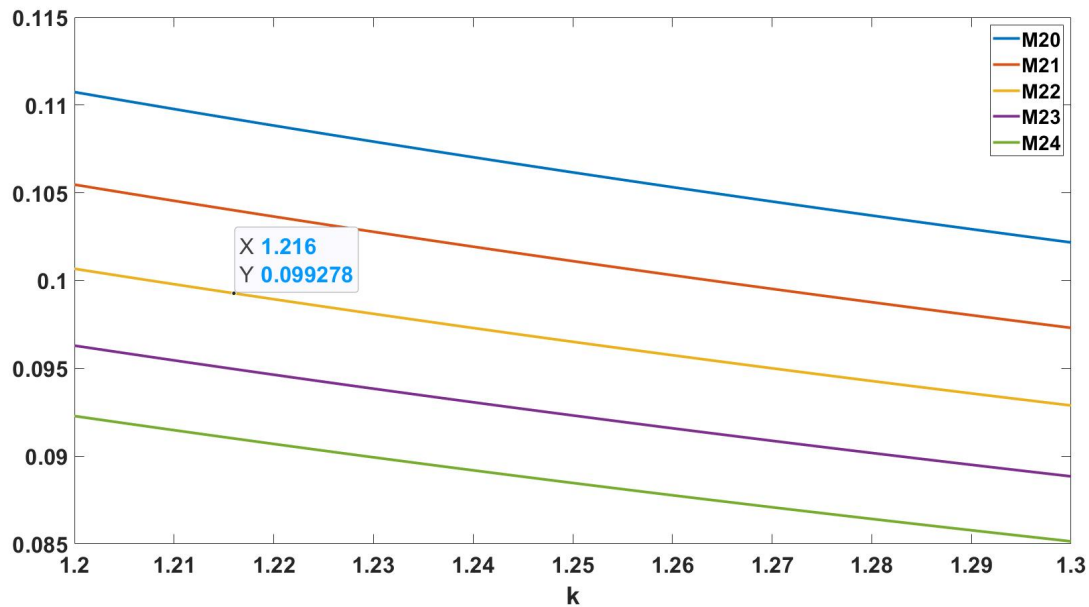


FIGURE 4.1: MATLAB plots of the right-hand side of Eq. 4.1 against values of k , for five values of \mathfrak{M}_{WF} in g mol $^{-1}$ shown in the legend, and an EFC of 70 %.

From Fig. 4.1 it can be seen that a k value of 1.216 for $\mathfrak{M}_{WF} = 22$ g mol $^{-1}$ results in a y-axis value close to 0.0993. Thus, $k = 1.216$ was chosen and used in subsequent calculations for the case of $EFC = 70\%$. Combining Eq. 3.10 and Eq. 3.11 and inserting $p_e = p_a = 9.455\dots \cdot 10^4$ Pa, $p_c = 1.5 \cdot 10^6$ Pa and $k = 1.216$, gives $\epsilon = 3.026\dots$. This multiplied with $A_t = 4.903\dots \cdot 10^{-5}$ m 2 then gives $A_e = 1.484\dots \cdot 10^{-4}$ m 2 .

The process up to this point was repeated for the two other EFC values, for all three cases of desired thrust, and the results - the values of A_t , A_e and ϵ - are summarised in Tab. 4.2.

TABLE 4.2: Nozzle cross-sectional throat and exit areas and their ratio, for different desired thrust levels and EFC values.

		EFC [%]								
		70			85			99.5		
		A _e [cm ²]	A _t [cm ²]	ε	A _e [cm ²]	A _t [cm ²]	ε	A _e [cm ²]	A _t [cm ²]	ε
Thrust [N]	100	1.484	0.490	3.027	1.435	0.484	2.963	1.500	0.514	2.918
	500	7.421	2.452		7.175	2.422		7.501	2.571	
	1000	14.841	4.903		14.351	4.844		15.002	5.142	

When analysing Tab. 4.2 it became apparent that the thrust chamber, in any case, will be quite small. In the cases of 100 and 500 N, the nozzle throat areas especially are very small and at those values - not larger than 2.5 cm² - the milling of the part would be problematic and the risk of breakage would be high. It was therefore decided to proceed with the design using a desired thrust value of 1000 N. Looking then at the EFC values, the differences between the cases are small and in all cases the ratio between the nozzle exit and throat areas is approximately 3. Maximising the amount of ethanol in the fuel mixture is desirable since that would suggest a larger amount of thrust being produced. However, when increasing the EFC the handling and storage risks increase and acquiring the fuel becomes more difficult. For these reasons, at least for this preliminary design, an EFC of 70 % was regarded to be sufficient.

To summarise, the preliminary propulsion system design will from here on assume a desired thrust level of 1000 N and an EFC of 70 % along with other parameter values previously presented for this specific case.

Inserting the two calculated nozzle areas for the selected case in Eq. 3.12 gives the following nozzle diameters: $D_t = 0.0249\dots$ m and $D_e = 0.0434\dots$ m. According to [15], the value of α should be no larger than 15 °. Assuming $\alpha = 15$ ° and using the calculated values of D_t and D_e in Eq. 3.16 gives $L_{div} = 0.0344\dots$ m.

4.2.2 Combustion chamber sizing

To calculate the volume of the combustion chamber Eq. 3.13 was used. The value of L^* typically ranges between 0.8 and 3 m according to [8]. Appropriate values to use for a GOx and hydrocarbon fuel WF rocket engine are in the range 1.27 - 2.54 m (50 - 100 in) according to [15] and the value used in the simulations in [43] is 1.0317 m. Taking these values into account, the value of L^* was assumed to be 1 m for simplicity and to approximate the simulations [43]. Using this, together with $A_t = 4.903\dots \cdot 10^{-4}$ m², in Eq. 3.13 gives $V_c = 4.903\dots \cdot 10^{-4}$ m³.

To determine the combustion chamber diameter and length, a similar method as the one used to determine the value of k was implemented. First, Eq. 3.12, Eq. 3.14 and Eq. 3.15 were rewritten and combined to get the following expression of V_c in terms of L_c and D_c :

$$V_c = \left(\frac{\pi D_c^2}{4} \right) \left(L_c + \left(\frac{D_c - D_t}{2 \tan \beta} \right) \left(1 + \left(\frac{2}{D_c} \right) \sqrt{\frac{A_t}{\pi}} + \frac{4A_t}{\pi D_c^2} \right) \right), \quad (4.2)$$

where $\beta = 60$ ° as suggested by [15]. With this value, and $A_t = 4.903\dots \cdot 10^{-4}$ m² and $D_t = 0.0249\dots$ m, Eq. 4.2 was plotted in MATLAB - several times for different values of D_c - against a range of L_c values and compared with the calculated value of $4.903\dots \cdot 10^{-4}$ m³ (see Fig. 4.2). The range of D_c values used was selected based on the suggestion that D_c "should be three to five times the nozzle

throat diameter so the injector will have useable face area" [15, p. 18]. The plots suggested several solutions of the set of parameter values for the given volume and a decision had to be made as to which solution would be the most suitable for this system. The largest chamber diameter considered - $D_c = 5D_t \approx 12.5$ cm - gives an approximate value of 0.4 cm for L_c , which did not seem like a practical solution. A decreasing chamber diameter entails an increasing chamber length and for $D_c = 3D_t = 0.0749\ldots$ m, $L_c = 0.0905$ m. This is the only option - for the considered parameter ranges - where the chamber length is larger than the diameter, which is also the case of the suggested design in [15]. It was therefore decided to use these two parameter values in this preliminary design.

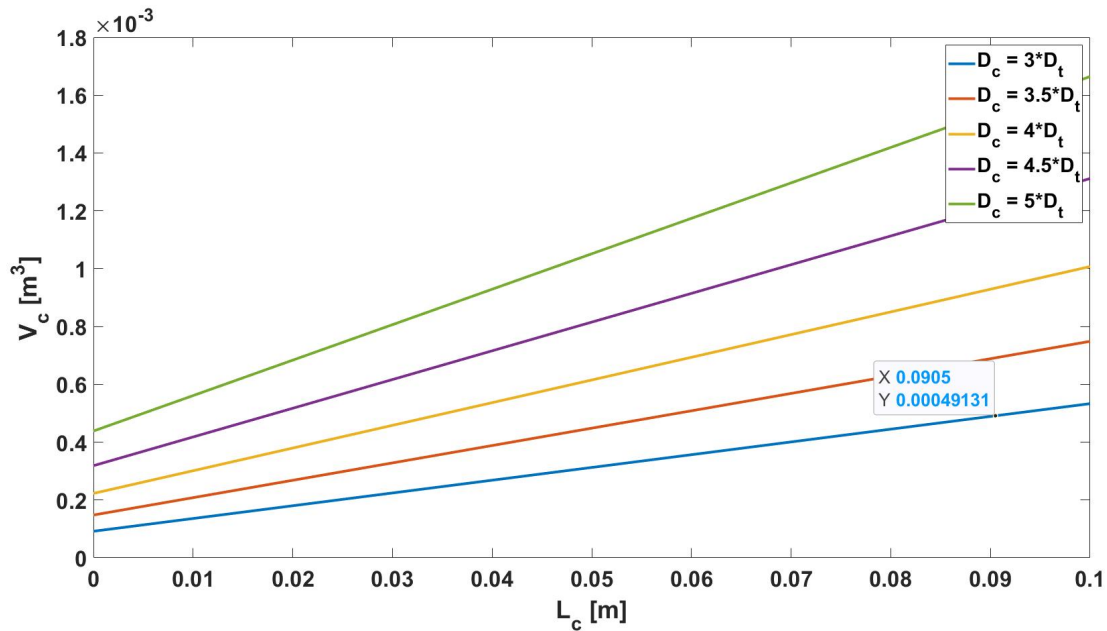


FIGURE 4.2: MATLAB plots of the combustion chamber volume, as defined in Eq. 4.2, against values of L_c for five values of D_c in terms of D_t as shown in the legend.

The combustion chamber cross-sectional area can be calculated with Eq. 3.12 rewritten and $D_c = 0.0749\ldots$ m, giving $A_c = 0.0044\ldots$ m². Sutton and Biblarz [8] suggest that A_c should be at least three times larger than A_t to avoid appreciable pressure losses in the thrust chamber that would lead to a decrease in system performance. When comparing the calculated values in this case, the ratio between the areas is nine which fulfills the criteria with a large margin. This further legitimises the choice of D_c .

Inserting $D_c = 0.0749\ldots$ m, $D_t = 0.0249\ldots$ m and $\beta = 60^\circ$ in Eq. 3.15 gives $L_{con} = 0.0144\ldots$ m.

4.2.3 Wall sizing and cooling

Thrust chamber and cooling jacket walls

The minimum thickness of the thrust chamber wall was calculated using Eq. 3.17. The chosen thrust chamber wall material is copper, for which $S_{cw} = 55.15 \cdot 10^6$ Pa (8000 psi) [15]. Inserting this with $p_c = 1.5 \cdot 10^6$ Pa and $D_c = 0.0749\ldots$ m in Eq. 3.17 gives $t_{cw, min} = 0.001\ldots$ m. The actual wall thickness should be greater to "allow for welding, buckling, and stress concentration" [15, p. 18] and a thickness approximately four times greater than the minimum is suggested. Therefore $t_{cw} = 0.004\ldots$ m.

The minimum thickness of the cooling jacket wall is determined in the same way as for the thrust chamber wall, however the jacket will be made out of another material and so the maximum allowable stress value is different. The material chosen is austenitic stainless steel of type SAE 316L. The maximum allowable (yield) stress for this steel type is $290 \cdot 10^6$ Pa [44]. Using this value in place of S_{jw} with $p_c = 1.5 \cdot 10^6$ Pa and $D_c = 0.0749\dots$ m in Eq. 3.26 gives $t_{jw, min} = 1.938\dots \cdot 10^{-4}$ m, in turn giving $t_{jw} = 4t_{jw, min} = 7.754\dots \cdot 10^{-4}$ m.

Coolant water

The two parameters that need to be determined for the water cooling process is the coolant mass flow rate and the size of the annular gap - between the outer surface of the thrust chamber and the inner surface of the cooling jacket - through which the coolant water will flow.

The coolant water mass flow rate can be found by solving Eq. 3.24 for \dot{m}_w and combining it with Eq. 3.25. This gives

$$\dot{m}_w = \frac{1.1\pi q_{cw}(D_c + 2t_{cw})L_c}{c_w \Delta T_w}. \quad (4.3)$$

The average heat transfer rate of copper is approximated, and the desired coolant water temperature rise value suggested, in [15] as $q_{cw} = 4.903\dots \cdot 10^6$ W m $^{-2}$ (3 Btu in $^{-2}$ s $^{-1}$) and $\Delta T_w = 278$ K (40 F) respectively. The value of c_w is 4190 J kg $^{-1}$ K $^{-1}$, as defined in [45]. Inserting these values together with $D_c = 0.0749\dots$ m, $t_{cw} = 0.004\dots$ m and $L_c = 0.0905$ m, in Eq. 4.3 gives $\dot{m}_w = 0.109\dots$ kg s $^{-1}$.

The annular coolant water flow gap can be described with the following equation, the result of combining Eq. 3.21, 3.22 and 3.23:

$$d_{gap} = \frac{\sqrt{\left(\frac{4\dot{m}_w}{\pi v_w \rho_w}\right) + (D_c + 2t_{cw})^2} - D_c - 2t_{cw}}{2}. \quad (4.4)$$

The coolant water flow velocity value is suggested in [15] as $v_w = 9.2$ m s $^{-1}$ (30 ft s $^{-1}$) and the mass density, $\rho_w = 998.2$ kg m $^{-3}$, can be found in [45]. Inserting these values, with $\dot{m}_w = 0.109\dots$ kg s $^{-1}$, $D_c = 0.0749\dots$ m and $t_{cw} = 0.004\dots$ m, in Eq. 4.4 gives $d_{gap} = 4.560\dots \cdot 10^{-5}$ m.

4.2.4 Propellant mass flow rates and injector properties

The total propellant mass flow rate can be calculated by solving Eq. 3.5 for \dot{m} and inserting $F_T = 1000$ N and $c = v_e = 2.236\dots \cdot 10^3$ m s $^{-1}$, giving $\dot{m} = 0.447\dots$ kg s $^{-1}$. Inserting this value and $r = 1.3$ in Eq. 3.7 gives $\dot{m}_f = 0.194\dots$ kg s $^{-1}$ and the oxidiser mass flow rate is then found by using Eq. 3.6 - $\dot{m}_o = 0.447\dots - 0.194\dots = 0.252\dots$ kg s $^{-1}$.

As it is highly recommended in [15], the fuel injector will consist of a commercial conical spray nozzle made out of brass. In order to acquire this nozzle the volume flow rate of the fuel \dot{V}_f had to be determined. The mass density of the fuel - an ethanol and water mixture with 70 % EFC - ρ_f is assumed to have a value of 0.885 kg dm $^{-3}$ = 885 kg m $^{-3}$, at a temperature of 293.15 K [46]. This, with $\dot{m}_f = 0.194\dots$ kg s $^{-1}$, gives $\dot{V}_f = 0.194\dots / 885 = 2.196\dots \cdot 10^{-4}$ m 3 s $^{-1}$ = $13.178\dots$ L min $^{-1}$. The selected nozzle is the 32885K151 brass spray nozzle from McMaster-Carr, with a full cone spray pattern - for uniform droplet distribution - and a spray angle of 120 ° [47]. At a pressure of $2.76 \cdot 10^6$ Pa (400 psi) it is capable of delivering $16.65\dots$ L min $^{-1}$ (4.4 gpm) of liquid, encompassing the calculated volume flow rate requirement.

Continuing with following the suggestions of [15], the GOx will be injected through four equally sized circular orifices, spread out equally on the injector face around the fuel injector nozzle and parallel to the combustion chamber centerline. The total oxidiser injection area was determined by calculating the oxidiser mass density at the injector with Eq. 3.19 and then inserting the value in Eq. 3.18. In order to do this, the ambient oxidiser mass density was calculated first with Eq. 3.20. The molecular mass of GOx is 32 g mol^{-1} [48]. To get the ambient pressure in atm, the calculated value in Pa was divided with the standard atmospheric sea-level pressure of 101325 Pa, giving $p_a = 9.455... \cdot 10^4 / 101325 = 0.933... \text{ atm}$. These values, with $R_u = 0.0821 \text{ L atm mol}^{-1} \text{ K}^{-1}$ and assuming an ambient temperature of 293.15 K, in Eq. 3.20 give $\rho_{o,a} = 1.240... \text{ kg m}^{-3}$.

The oxidiser pressure at the injector is the drop in pressure over the injector added to the combustion chamber pressure p_c [15]. According to [15], the injection pressure drop is commonly between $0.482 \cdot 10^6$ and $1.034 \cdot 10^6 \text{ Pa}$ (70 - 150 psi). Assuming the highest value in the range for the pressure drop gives $p_{inj} = p_c + 1.034 \cdot 10^6 = (1.5 + 1.034) \cdot 10^6 = 2.534 \cdot 10^6 \text{ Pa}$. Inserting this, with $p_a = 9.455... \cdot 10^4 \text{ Pa}$, $\rho_{o,a} = 1.240... \text{ kg m}^{-3}$ and assuming the temperature at the injector is 293.15 K [15] in Eq. 3.19 gives $\rho_{o,inj} = 33.251... \text{ kg m}^{-3}$.

The value of C_d can be assumed to be 0.7 [15]. Inserting this, together with $\dot{m}_o = 0.252... \text{ kg s}^{-1}$, $\rho_{o,inj} = 33.251... \text{ kg m}^{-3}$ and $\Delta p = 1.034 \cdot 10^6 \text{ Pa}$, in Eq. 3.18 gives $A_o = 4.353... \cdot 10^{-5} \text{ m}^2$. Since four oxidiser injection holes will be used, the cross-sectional area per hole is $A_{inj} = A_o / 4 = 4.353... \cdot 10^{-5} / 4 = 1.088... \cdot 10^{-5} \text{ m}^2$. Using Eq. 3.12, the diameter of each injection hole is $D_{inj} = 0.003... \text{ m}$.

Important to note here is that the injection hole size was calculated assuming an ambient temperature of 293.15 K. Were this rocket engine to be operated at another ambient temperature - or at another ambient pressure - the oxidiser mass flow rate would have to be regulated accordingly in order to achieve the same performance.

4.2.5 Ignition assembly

The selected propellants are non-hypergolic, meaning an external heat source is required for ignition. It was decided to implement a simple yet reliable ignition solution for this propulsion system. Namely the hot-source ignition method recommended in [15]. In this method, an ignition coil - or spark coil - is used to create a spark between the exposed ends of two insulated wires. Close to the gap between the wires, while keeping the ends clear, a small piece of gasoline-soaked cotton is attached. The assembly is then inserted into the lower end of the combustion chamber through the nozzle throat and attached. During a test, a small flow of GOx is allowed to pass the wires and cotton piece. Then the ignition coil is energised and a spark is created between the wire ends, which sets the cotton on fire. The burning cotton, together with the flow of GOx, subsequently ignites the fuel when this is sprayed into the chamber [15].

The ignition coil works as a step-up transformer where a relatively small input voltage is converted into several thousands of volts in order to generate a spark. Its main parts are two coils of wire - one primary coil with hundreds of turns of wire and one secondary with several thousand turns - both wrapped around a single iron core. First, the positive terminal of a DC power supply is connected to one end of the primary coil by closing a switch, with the other end being connected to the negative terminal. This sends current through the coil, building up a magnetic field around both coils. If the switch is opened the generated magnetic field collapses which induces a large current in the secondary coil. This current is subsequently led through the secondary coil and out of the induction coil component via one of the insulated wires of the assembly. When reaching the exposed end of the wire the current creates a spark between it and the other wire, which is connected to ground. As the field collapses a surge of electricity is also led back towards the switch via the primary coil. To avoid the creation of another damaging spark over the switch, a capacitor is placed in parallel with it

to absorb the electricity. A cross-section of the ignition coil and an illustration giving an idea of what the ignition assembly will look like are displayed in [49].

The selected ignition coil is the oil-filled 12V ignition coil from Biltema [50]. The reason for choosing a more conventional can-type ignition coil, as opposed to the more modern type, is that it has a simplistic design providing uncomplicated wire connections. Most modern ignition coils are electronically controlled, has more advanced designs for better ignition performance in specific car models and are in general more expensive. The remaining components of the ignition assembly to be selected and acquired are a 12V power supply, a switch that can be electronically controlled, a capacitor with a large enough capacitance value and insulated wires to connect everything similarly to the diagram in [49].

4.2.6 Thrust chamber design summary

Fig. 4.3 shows a drawing of the preliminary thrust chamber design, with calculated and rounded physical parameters. Tab. 4.3 presents the calculated and rounded values of all mass flow rate parameters.

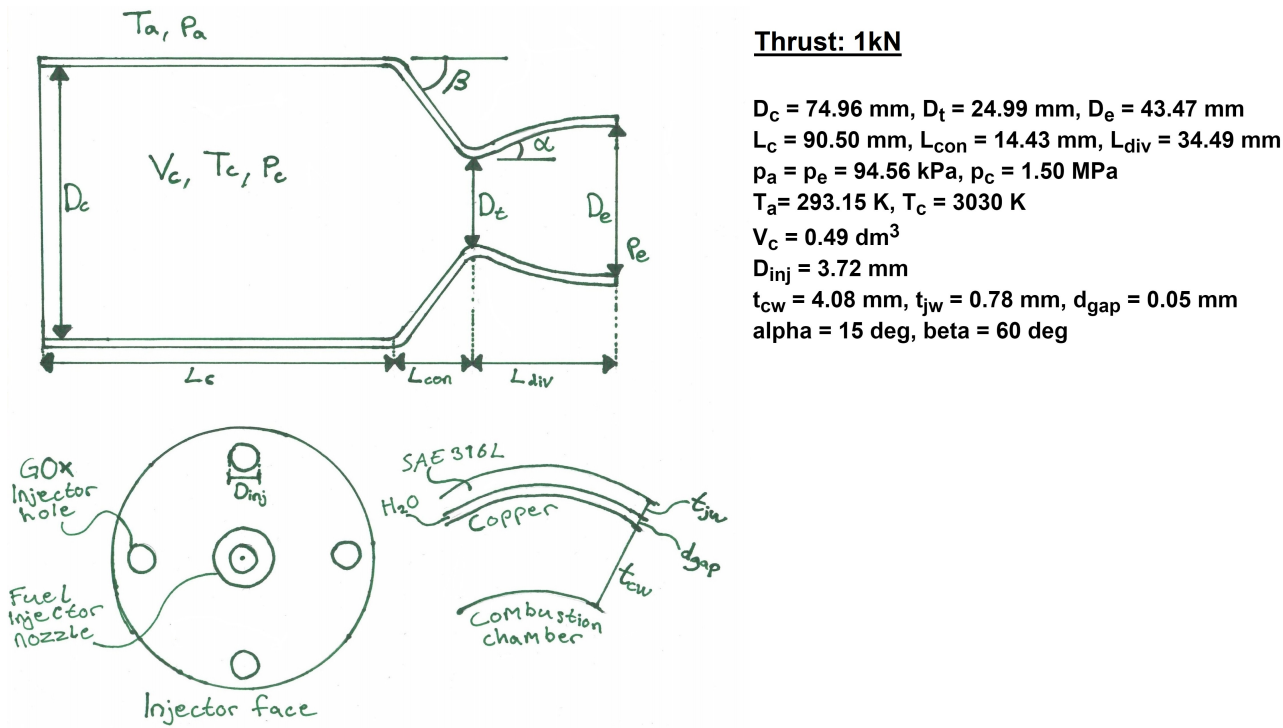


FIGURE 4.3: Drawing of the preliminary physical design of the thrust chamber. Also shown are the calculated and rounded physical parameter values. The drawing is based on similar drawings found in [8] and [15].

TABLE 4.3: Calculated and rounded values of the mass flow rate parameters in kg s^{-1} .

\dot{m}	\dot{m}_f	\dot{m}_o	\dot{m}_w
0.447	0.194	0.253	0.109

4.3 Propellant feed assembly

In this propulsion system design, a regulated gas pressure fed propellant feed assembly - with a separated Gaseous Nitrogen (GN2) supply for fuel loading - is implemented. All components selected to be used in the presented design were chosen based on design recommendations in [15] and a comparative study done by the author of this report, of available parts and units on the market with properties following the design specifications. Suggestions for some companies and units to include in the study, as well as various design suggestions, were given to the author by various project advisors and the project supervisor.

Due to the risks that come with operating a propulsion system, many operations must be done remotely to increase system safety. For this reason - whenever applicable - components permitting electrical actuation and digital read-out were selected instead of manual counterparts.

During combustion, due to the dynamic pressure, the thrust chamber is expected to experience quite large vibrations. However, the framework yet to be designed is assumed to be stable enough and designed in such a way that vibrations will not spread to, or be an issue for, the remaining components part of the assembly. Thus, vibration resistance has not been specifically reviewed - nor considered to be of great importance - in the component selection process, apart from the selection of the thrust chamber PSs as seen below.

All components - except for the thrust chamber and fuel tank - are Commercial Off-The-Shelf (COTS) type components. Therefore, components should be able to be replaced with relative ease when they become damaged and if some selected units would go out of production, suitable variants should not be difficult to acquire. The number of system uses before failure hence depends on the life time of individual components, however this is not something that has been investigated further as part of this master thesis project.

The schematic diagram of the assembly, shown in Fig. 4.4, is based on similar diagrams found in [15] and [34].

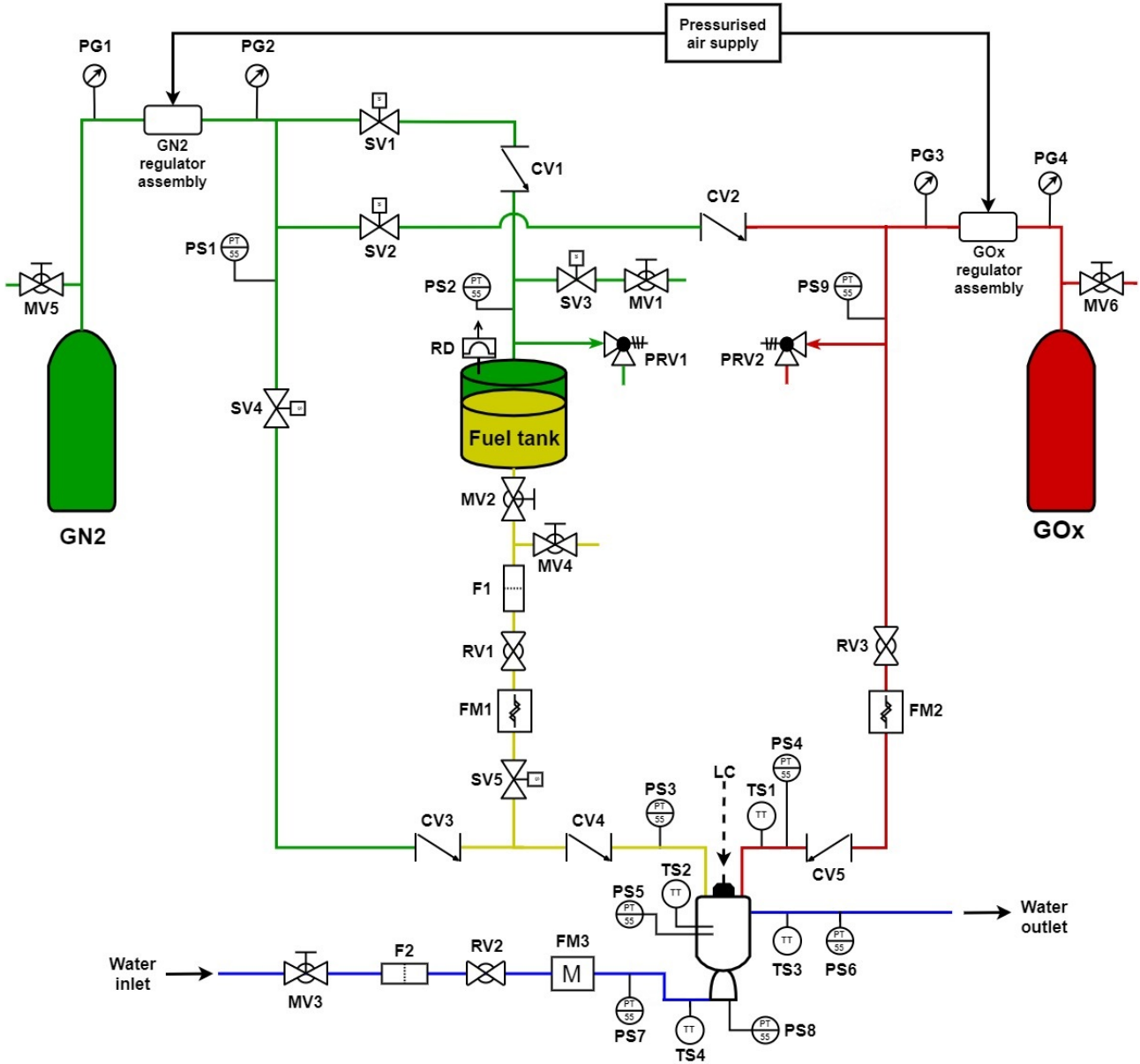


FIGURE 4.4: Schematic diagram of the propellant feed assembly design. Green - GN2, Red - GOx, Yellow - Ethanol, Blue - Coolant water. CV(n) - Check Valve, F(n) - Filter, FM(n) - Flow Meter, LC - Load Cell, MV(n) - Manual Valve, PG(n) - Pressure Gauge, PRV - Pressure Relief Valve, PS(n) - Pressure Sensor, RD - Rupture Disk, RV(n) - Regulating Valve, SV(n) - Solenoid Valve, TS(n) - Temperature Sensor. Symbols used in the diagram for valves, sensors etc. are standard Piping and Instrumentation Diagram (P&ID) symbols found in [51].

As can be seen in Fig. 4.4, the assembly is divided into four main sections - a GN2 section, a fuel section, a GOx section and a coolant water section for the thrust chamber cooling. The ethanol fuel and the GOx are fed to the thrust chamber injector through separate plumbing sections. The GN2 supply is used mainly for the pressurisation of the fuel tank in order to feed the fuel to the thrust chamber. It is also used for the purpose of purging the fuel and oxidiser sections of propellant residues after a test, in order to achieve maximum feed line cleanliness for handling safety and to assure accurate future tests. Therefore, additional plumbing sections from the GN2 supply have been included to allow this function. Specific components referred to in this section can all be found in this figure.

4.3.1 Fuel tank

To calculate the required fuel tank volume V_f , Eq. 3.27 was used. For this design, a desired test burn time of 60 s was selected, as suggested by the project supervisor. Inserting this, with $\dot{V}_f = 2.196\ldots \cdot 10^{-4} \text{ m}^3 \text{ s}^{-1}$, in Eq. 3.27 with a design factor of 1.5 gives $V_{\text{tank}, f} = 0.0197\ldots \text{ m}^3 \approx 20 \text{ L}$.

The fuel tank will be made of stainless steel. With an operating pressure of $p_{f, op} = 3.5 \cdot 10^6 \text{ Pa}$ (500 psi) - which is the pressure used for the design example of the fuel tank in [15] - a design pressure two times this value ($7 \cdot 10^6 \text{ Pa}$) will be used for the tank design. The tank will have three ports in total, two in the top end and one in the bottom. One of the top end ports will be used to fit a rupture disk. The other will serve several functions, namely filling the tank with fuel, pressurising it with GN2, venting the GN2 after a test and to quickly relieve the pressure if needed. The bottom end port will be used to empty the tank of fuel, either feeding it forward towards the thrust chamber during tests or removing it from the feeding line into a separate container if required.

The design parameters will be given to a professional company specialising in building pressure vessels, which will then build the tank while making the necessary decisions on tank shape and wall thickness to comply with the specifications and pressurised container regulations.

4.3.2 Pressurised gas tanks

Both the GOx and the GN2 supply will consist of ready-made, highly pressurised gas cylinders. The minimum required tank volume for the GOx was calculated with Eq. 3.27. To find \dot{V}_o , the GOx density within the tank had to be determined using Eq. 3.28. The pressure in the tank was assumed to be a common filling pressure for commercially available gas containers - 200 bar - or 197.4 atm, while the temperature was assumed to be 293.15 K. These values, with $\mathfrak{M}_o = 32 \text{ g mol}^{-1}$ and $R_u = 0.0821 \text{ L atm mol}^{-1} \text{ K}^{-1}$, in Eq. 3.28 give $\rho_{o, \text{tank}} = 262.4\ldots \text{ kg m}^{-3}$. This value with $\dot{m}_o = 0.252\ldots \text{ kg s}^{-1}$ then gives $\dot{V}_o = 0.252\ldots / 262.4\ldots = 9.628\ldots \cdot 10^{-4} \text{ m}^3 \text{ s}^{-1}$. Inserting this value together with $\text{time}_{\text{test}} = 60 \text{ s}$ in Eq. 3.27, again with a design factor of 1.5, gives $V_{\text{tank}, o} = 0.086\ldots \text{ m}^3 \approx 87 \text{ L}$. It was decided to use two tanks of 50 L each for the oxygen supply, to cover the required volume. The selected GOx cylinder is the ODOROX® 50L cylinder from AGA [52], pressurised at 200 bar. As an added safety feature, the cylinder contains dimethyl sulphide so that any GOx leaks are revealed by the additive's distinct odour.

The minimum required tank volume for the GN2 was calculated in a different way, using Eq. 3.29. By closing and opening certain valves, the GN2 supply, the fuel tank and the feed line section in between can together be seen as a closed system in the ideal case. The temperature in this closed system is assumed to be constant. In this case, Boyle's law can be applied in order to calculate the volume. The volume occupied by the GN2 inside the fuel tank increases throughout a test as the fuel is depleted. Taking the fuel tank in the state where all fuel has been replaced by GN2 as location two - that is $p_{l2} = p_{f, op}$ and $V_{l2} = V_{\text{tank}, f}$ - and the GN2 supply tank(s) as location 1 - $p_{l1} = p_{GN2}$ and $V_{l1} = V_{GN2}$ - Eq. 3.29, with 1.5 as the design factor, can be rewritten as

$$V_{GN2} = 1.5 \cdot \frac{p_{f, op} \cdot V_{\text{tank}, f}}{p_{GN2}}. \quad (4.5)$$

Assuming the GN2 pressure is 200 bar = $20 \cdot 10^6 \text{ Pa}$ and inserting $p_{f, op} = 3.5 \cdot 10^6 \text{ Pa}$ and $V_{\text{tank}, f} = 0.0197\ldots \text{ m}^3$ in Eq. 4.5 gives $V_{GN2} = 0.005\ldots \text{ m}^3 \approx 5 \text{ L}$. This is however only the required volume to feed all fuel from the fuel tank and a larger volume will be needed, taking into account the function of flushing the assembly with GN2 after a finished test. To account for this, a supply of approximately four times the calculated volume will be used. Specifically, the 20L GN2 cylinder from AGA [53]

pressurised at 200 bar was selected. Future tests with the finished platform will determine if this volume is sufficient, if it needs to be increased or if it can be decreased while still allowing the same system performance.

4.3.3 Plumbing

For the plumbing, stainless steel tubing with metal-to-metal seat fittings will be used, as comes recommended in [15]. Specifically, the tube unions by DILO [54] have been selected for the fittings, due to their efficient metal-to-metal sealing principle. The GN2, fuel and coolant water tubing sections will have the size DN8 (1/4 in) and the GOx section size DN10 (3/8 in). The GOx tubing, along with any other components or parts coming into contact with the GOx, must be thoroughly cleaned specifically for oxygen service. This is due to the increased risk of combustion with most materials that the use of GOx entails [15].

4.3.4 Flow control components

Valves

Five types of valves are used in the assembly; solenoid valves, manual valves, check valves, flow regulating valves and pressure relief valves.

Solenoid valves are used for the valves which are either in open or closed position during operation and which are not to be manually operated for safety purposes. SV1 is the GN2 fuel tank feed valve, SV2 and SV4 are the GN2 purge valves, SV3 is the GN2 vent valve and SV5 is an emergency shut-off valve, used in case a test needs to be prematurely ended and the fuel flow quickly stopped. For these valves the Series 262 direct acting 2 way solenoid valve from ASCO, in stainless steel and with size DN8 (1/4 in), will be used. In case of a power loss during operation, to avoid pressure build-up and uncontrolled rocket engine burning, the automated system response will be to stop the fuel flow and purge the feed lines with GN2 while simultaneously venting them in order to depressurise the system. Therefore, to close off the fuel feed line at power loss, SV5 will be of the normally closed type - specifically the 8262H080 model, rated up to $5.17 \cdot 10^6$ Pa (750 psi) of pressure [55]. The remaining SVs will be of the normally open type - specifically the 8262H130 model, rated up to $4.48 \cdot 10^6$ Pa (650 psi) of pressure [56] - so that all propellant feed lines are automatically purged and vented in case of power loss. The valve models were chosen because they are rated for more than the system operating pressure and can withstand corrosive liquids as well as inert gas (GN2).

Manual valve MV1 will be used to fill the fuel tank with ethanol while solenoid valve SV3 is kept open. SV3 is then closed during tests and opened when the GN2 is to be vented from the fuel tank and the connected tubing section. MV1 will be opened before combustion tests. MV2 and MV3 are included to make it possible to close off the fuel and coolant water sections from their respective supplies, so that the functionality of downstream components can be tested before a combustion test. MV4 will be used to drain the fuel section if required. MV5 and MV6 are used to vent the upstream sections of the pressurised gas regulators, once the downstream sections have been purged and vented. By recommendation in [15], the selected manual valve for MV1, MV2, MV3 and MV4 is a stainless steel ball valve with Teflon seats. Namely the Series 59 full-port ball valve from Flowserve Worcester Controls [57] of size DN8 (1/4 in), with an all stainless steel three-piece configuration and screw end connections. For media temperatures up to 38 °C (100 °F), the valve type is rated for approximately $6.9 \cdot 10^6$ Pa (1000 psi). Due to the higher pressure of the gas regulator upstream sections, another type of valve will be used for MV5 and MV6. Specifically, the SK Series multipurpose ball valve from Swagelok [58] was selected for these two valves, size DN8 (1/4 in) for the GN2 section and

DN10 (3/8 in) for the GOx section. This valve model is rated for up to 413 bar - more than double the pressurised gas cylinder pressure. It contains parts of stainless steel, PolyEther Ether Ketone (PEEK), Fluorocarbon FKM and PolyTetraFluoroEthylene (PTFE) which are all compatible with both GOx and GN2 according to [59]. The GN2 and GOx cylinders come with manual valves included.

The **check valves** are used to restrict the fluid flows to go in only one direction. It was important to find a valve model which can withstand all fluids in use in the system and has metal-to-metal seats, as suggested in [15]. Additionally, since some of the valves will be used with oxygen, the selected type must have only oxygen compatible parts. The selected component is the CP Series check valve from Swagelok [60] with a fixed cracking pressure, or inlet pressure at first flow occurrence, of $6.89 \cdot 10^3$ Pa (1 psi). It has a simple one-piece design, consists of stainless steel and Fluorocarbon FKM parts and has a pressure rating of $15 \cdot 10^6$ Pa at maximum temperature (190 °C) and $20.6 \cdot 10^6$ Pa at room temperature (37 °C). For CV1, CV3 and CV4, the SS-4CP2-1 model of size DN8 (1/4 in) was selected and for CV2 and CV5, the SS-8CP2-1 model of size DN15 (1/2 in) [61] [62].

The **flow regulating valves**, or control valves, are arguably the most important of the flow control components as they directly influence the thrust profile. It was important to find a valve model which can be electronically and remotely actuated, as well as providing precise control, while still being able to handle the relatively high pressure levels of the assembly. After getting a company recommendation from a project advisor - Vanderlei Neias at Edge of Space - and some additional research by the author, the CPT type floating ball rotary control valve by Flowserve Worcester Controls was chosen. The CPT type, or characterised seat control valve, has the advantage of providing high precision flow control due to the customisable shapes of the valve port seats. Furthermore, the floating ball design concept, together with the specific materials used, makes bubble tight valve shutoff possible [63].

For the coolant water regulating valve RV2, the CPT 44 model of size DN8 (1/4 in) was selected. For the valves controlling the flow of the more hazardous fluids - the fuel and GOx valves RV1 and RV3 - another model was selected, namely the CPT 94. This valve model includes an improved sealing solution around the valve stem to reduce fugitive emissions due to leaks. RV1 will be of size DN8 (1/4 in) and RV3 size DN15 (1/2 in). The chosen material for the valve port seats of both valve models is the characterised "Metal A" - sintered stainless steel impregnated with TetraFluoroEthylene (TFE). The body, stem and ball of the valves are made of stainless steel and the ball is nickel-coated. All three valves will have a three-piece valve configuration with screw end connections. Both CPT 44 and CPT 94 are rated for approximately $9.8 \cdot 10^6$ Pa (1425 psi) which is well above the operating pressure [63].

Each valve will be controlled with an electric actuator. As it comes recommended in [63] for computer control purposes, the Flowserve Worcester Controls Series 75 Electric Actuator [64] was selected. The valve actuators were sized by following the instructions in the Worcester Controls Actuator Sizing Manual [65], where the required valve torque is determined based on valve design, application and maximum differential pressure across the valve. The torque value is then compared to the startup torques of various actuators, in order to determine the final actuator size to use. Standard water inlet pressure is somewhere in the range of 40 - 60 psi. Using 70 psi as the worst case differential pressure across RV2 led to the choice of a size 10 actuator for this valve. For the remaining valves, a worst case differential pressure of 500 psi - equivalent to the operational pressure - was used, giving an actuator of size 12.

The actuators will receive positioning inputs from an electronic positioner, namely the DataFlo P™ Positioner - DFP 17 - from Flowserve [66]. This positioner was chosen because it is optimised for digital, remote control of the series 75 electric actuator. It is controlled by a microcontroller and offers calibration, monitoring and diagnostics of the regulating valve setup from a control room.

The **pressure relief valves** are used as a safety measure to prevent the fuel tank and GN2 feed line - or the GOx feed line - from bursting, should the internal pressure increase to unexpected levels.

The selected relief valves will be from the RVC05-Npt stainless steel high pressure relief valve series from Straval [67], of the low pressure group with a pressure rating of $10.34 \cdot 10^6$ Pa (1500 psi) and PTFE seats. The reasons for choosing this valve type are that their wetted parts are made from the preferred material - stainless steel, they come in a variety of sizes to accommodate the different plumbing sizes of the assembly and they are spring-loaded with an adjustable relief pressure - which is recommended in [15]. It is an advantage to be able to adjust the relief pressure, as the value to set depends on the operational pressure in a certain use case, as well as the maximum pressures for different components. For the current system design, the operational pressure is $3.5 \cdot 10^6$ Pa and the design pressure of the fuel tank $7 \cdot 10^6$ Pa. Which specific relief pressure to set PRV1 and PRV2 to has not yet been decided, however for this case it will be a value somewhere between these two values, and so the selected models have ranges encompassing them. For PRV1, the RVC05-02T of size DN8 (1/4 in) with a set relief pressure range of $0.86 \cdot 10^6$ – $7.58 \cdot 10^6$ Pa (125-1100 psi) was selected. For PRV2, the selected model is the RVC05-03T of size DN10 (3/8 in) with a set relief pressure range of $1.03 \cdot 10^6$ – $8.62 \cdot 10^6$ Pa (150-1250 psi).

In addition to PRV1, a rupture disk will be fitted to the fuel tank so as to increase the system safety, in case the relief valve should fail. As they provide a wide range of rupture disks and accessories, it was decided that a disk from ZOOK will be used for this purpose, by recommendation from a project advisor - Olle Persson at LTU. After some discussions with company representatives and distributors [68], a disk and holder assembly with a burst pressure close to the fuel tank design pressure was selected. Namely, the ZOOK Pre-Bulged Forward-Acting DN8 (1/4 in) stainless steel rupture disk - with a burst pressure of $7 \cdot 10^6 \pm 10\%$ Pa at 20°C - together with the ZOOK DN15 (1/2 in) stainless steel inlet screw type angle seated disk holder [69] [70] [71].

Pressure regulator assemblies

The regulation of the GOx and GN2 pressure to a constant downstream pressure is one of the operations that needs to be done remotely, to minimise risk, and so remotely controlled actuators will be used to open and close the regulator valves. Each regulator assembly will consist of three main components; (1) a pneumatically actuated control valve used for decreasing the high pressures of the gas supply sections to the operating pressures of downstream sections, (2) a Proportional–Integral–Derivative (PID) controller used to automatically regulate the outlet pressures to a set point value based on continuous downstream pressure measurement input and (3) a pressure transmitter mounted downstream of the control valve, measuring the pressure level and sending a proportional signal to the PID controller for comparison with the set point value.

The selected component for the control valves is the high pressure and severe service type 1711, equal percentage, normally closed globe control valve from Badger Meter Research Control Valves (RCV) [72], of size DN25 (1 in) with a pressure rating of $34.5 \cdot 10^6$ Pa (345 bar) at 24°C . It is made of stainless steel inlaid with stellite - an alloy with "high wear resistance and superior chemical and corrosion performance in hostile environments" [73], consisting of Cobalt, Chromium and various other materials. The GOx regulator valve will be cleaned for GOx use. According to performed valve calculations [74], the selected valve model can handle an inlet pressure of 200 bar and will be able to deliver the operating outlet pressure of $3.5 \cdot 10^6$ Pa (35 bar). Also in [74], for the GOx regulator valve, a mass flow rate range of 0.07 - 0.26 kg s^{-1} has been calculated, which encompasses the calculated value displayed in Tab. 4.3; $\dot{m}_o = 0.253 \text{ kg s}^{-1}$. A mass flow rate range of 0.04 - 0.2 kg s^{-1} for the GN2 regulator valve has also been calculated [74], however no expected mass flow rate for this media to compare with has been calculated by the author of this thesis. On the other hand, the calculated fuel mass flow rate is $\dot{m}_f = 0.194 \text{ kg s}^{-1}$, as seen in Tab. 4.3, and the GN2 value is not expected to exceed this.

Each control valve will be actuated by the Badger Meter RCV type PA35 multi-spring, Air To Open (ATO), stainless steel pneumatic actuator [75], rated at $4 \cdot 10^5$ Pa (4 bar) at 21 °C. Connected to the actuator is a current to pressure (I/P) transducer. This component controls the actuator by converting an analog 4 - 20 mA current control signal coming from the PID controller to a 0.2 - 1 bar control pressure, which is subsequently sent to the actuator. The I/P transducer requires a pressurised air supply at 1.4 bar. Also included is a filter regulator used to filter the incoming transducer air flow from contaminants and regulate the pressure. The control valve, actuator, I/P transducer and filter regulator will be delivered as one unit, connected together. An electrical actuator would have been preferred to a pneumatic type, in order to avoid the need of a pressurised air supply for its operation, however the forces required to operate the valves will be too large for an electronic type [74].

The selected pressure transmitter model for the regulator assemblies is the GEFRAN type TK-E-1-Z-B04D-M-V pressure transmitter made of stainless steel alloys, with a measurement range of $0 - 4 \cdot 10^6$ Pa (0 - 40 bar) and rated for up to $8 \cdot 10^6$ Pa (80 bar) [76]. The transmitter will send an analog 4 - 20 mA current signal, proportional to the measured pressure, as one of the inputs to the PID controller - the PCS-PID-AGD controller from Pressure Control Solutions [77], specifically. The PID controller will send an analog 4 - 20 mA current signal to the actuator to continuously change the regulator valve passage size, depending on the difference between the measured outlet pressure and the set point pressure value. The set point value is delivered via RS-232 communication from the operator station [74].

Filters

Two filters - F1 and F2 - will be used in the assembly, to remove any debris or contaminants from the fuel and coolant water. The fuel filter is especially important as particles in the fuel could easily block the fuel injector nozzle. The selected filter is the stainless steel high-pressure inline filter 9811K86 from McMaster-Carr [78], able to filter particles down to 10 microns as recommended in [15]. It has good corrosion resistance and is rated for $20.7 \cdot 10^6$ Pa (3000 psi) of pressure.

4.3.5 Parameter measurement components

The parameter types that are to be measured is the rocket engine thrust level, mass flow rate, pressure and temperature.

Thrust

The thrust will be measured with a load cell connected to the top of the thrust chamber assembly. The Kistler strain gage load cell type 4578A10C3 [79], capable of measuring forces up to 10000 N, was selected for this component. It is simple to mount, has good accuracy and the large measuring range makes the component usable for future tests with other types of rocket engines capable of larger thrust production.

Mass flow rate

The fuel, oxidiser and coolant water mass flow rates are measured with FM1, FM2 and FM3 respectively. For FM1 and FM2, the selected component is the Proline Promass F 300 Coriolis flowmeter from Endress+Hauser of size DN15 (1/2 in) [80], rated up to $10 \cdot 10^6$ Pa (100 bar) [81]. For FM1, a model with wetted parts made of stainless steel and a mass flow rate operating range of 0 - 1.806

kg s^{-1} was selected. FM2 will have a mass flow rate operating range of $0 - 1.092 \text{ kg s}^{-1}$. The material to be used for the wetted parts of FM2 is Alloy C22 - an alloy of Nickel, Chromium, Molybdenum and Tungsten, chosen because of its good resistance to various oxidising media, e.g. GOx [82]. The selected model will also be cleaned specifically for GOx usage. The selected component for FM3 is the Proline Promag H 300 Electromagnetic flowmeter from Endress+Hauser of size DN8 (1/4 in) [83], rated up to $4 \cdot 10^6 \text{ Pa}$ (40 bar) with wetted parts of stainless steel with a PerFluoroalkoxy Alkane (PFA) liner and a mass flow rate operating range of $0.002 - 0.5 \text{ kg s}^{-1}$ [81].

According to Tab. 4.3, the fuel mass flow rate is $\dot{m}_f = 0.194 \text{ kg s}^{-1}$, the GOx mass flow rate $\dot{m}_o = 0.253 \text{ kg s}^{-1}$ and the coolant water mass flow rate $\dot{m}_w = 0.109 \text{ kg s}^{-1}$. Also, the operational pressure of the fuel and GOx sections of the assembly is $3.5 \cdot 10^6 \text{ Pa}$ (35 bar) and the maximum expected coolant water section pressure is $0.48 \cdot 10^6 \text{ Pa}$ (70 psi). Comparing these values with the mass flow rate and pressure ranges of the selected components indicates that they fulfil the requirements.

Pressure

The pressure level in different sections of the assembly will be measured with either electrical pressure sensors or pressure gauges. The sensors are used for remote pressure monitoring during tests. The gauges are used in the sections close to the highly pressurised gas cylinders as a safety feature, so that these critical pressure levels can be checked directly whenever an operator is in close proximity to the assembly. This allows the operator to confirm if the system is or is not pressurised before replacing empty gas cylinders for example.

For the pressure gauges, the selected component is the WIKA 100mm in diameter, stainless steel Bourdon tube gauge with a pressure display range of $0 - 60 \cdot 10^6 \text{ Pa}$ (0-600 bar) [84]. Using a Bourdon tube type for this component is recommended in [15]. The 100 mm display window, together with the selected display range, will make the measured pressure up to 200 bar clearly distinguishable to the operator. According to [84], the selected gauge type is rated for a maximum of $60 \cdot 10^6 \text{ Pa}$ in static pressure load and up to $54 \cdot 10^6 \text{ Pa}$ in dynamic load. Additionally, the selected model is cleaned specifically for GOx service.

The type of electrical pressure sensor to use depends on the type of pressure that is to be measured, namely dynamic or static, which are in turn depending on the properties of the measured fluid. The former is proportional to the square of the fluid velocity. In most cases dynamic pressure is negligible compared to the static kind, due to the relatively low fluid velocities in most plumbing or pressure vessels [85]. It is the understanding of the author that the fluid velocities in the feed assembly plumbing will be relatively low, compared to within the thrust chamber where they will be much higher. Thus, a decision was made to use a sensor technology aimed for dynamic pressure measurements for PS5 and PS8 and one aimed for static measurements for the remaining PSs in the system.

For PS5 and PS8, the piezoelectric pressure sensor 603CAA in stainless steel from Kistler [86], with a pressure range of $0 - 100 \cdot 10^6 \text{ Pa}$ (0-1000 bar), was selected. This sensor model was chosen because it is specifically suited for highly dynamic pressure measurements due to a high natural frequency. Furthermore, the specific model is acceleration compensated which "ensures reliable measurements even under highly vibrating conditions" [86, p. 1]. This is important for the thrust chamber measurements during combustion tests. The PE version of this sensor was selected instead of the IEPE version - or the version with charge output was selected instead of the voltage output version - because the PE version is able to measure not only dynamic pressure but also quasi-static pressure (true static pressure measurements are not possible with this sensor technology) [87]. As mentioned, it is expected that the pressures in the thrust chamber will be dynamic, however having the option for quasi-static measurements is good in case some static pressure is seen as well. It is possible that other

types of sensors will be needed in the thrust chamber in the future, for parallel static measurements, if this pressure type should prove to be more considerable than expected.

Due to the extreme combustion chamber temperatures - expected to reach values around 3030 K, some special measuring solution will have to be implemented for pressure sensors PS5 and PS8 as the 603CAA sensor is only rated up to 473.15 K (200 °C). By suggestion from a project advisor - Anna Lind at GKN Aerospace - this could be done in two ways. Either by moving the sensors further from the combustion chamber within open ended tubes - to a point where the temperatures are lower - and/or encasing the sensors in isolating adapters so that pressure can be measured close to the chamber while still withstanding the high temperatures. The former method is used for static pressure measurements and the latter for dynamic, meaning the latter needs to be implemented for the thrust chamber design in this case.

For the remaining PSs, a piezoresistive pressure transmitter - namely the M6 absolute pressure transmitter, type 4080B130 in stainless steel from Kistler [88] - was selected, as this sensor technology is optimal for static pressure measurements [86]. The specific component was chosen because it can measure pressures up to $13 \cdot 10^6$ Pa (130 bar), well above the operating pressure. Although the static pressures in the feed lines are expected to be much more prominent than the dynamic, small dynamic pressures could still occur. Therefor, another reason for choosing this specific component is that it is "suitable for various demanding Test & Measurement applications where static pressures or dynamic pressures up to 5 kHz need to be measured" [88, p. 1].

Temperature

For all temperature sensors except TS2, the resistance temperature detecting immersion type probe S604PD40Z120T made of stainless steel from Minco [89] will be used. This sensor probe offers rapid response to changes in temperature, has a pressure rating of $10.3 \cdot 10^6$ Pa (103 bar) - well above the operating pressure - and can measure temperatures up to 533.15 K (260 °C).

Since TS2 needs to measure much higher temperatures within the combustion chamber, another type of temperature measuring device will be used for this component. Again by suggestion from Anna Lind, it was decided that using a thermographic - or Infrared Radiation (IR) - camera would be a good choice for this purpose. These cameras can display very high temperatures with precision, without having to be close to the combustion chamber itself. The temperatures measured with this type of camera are the outside surface temperatures of the chamber. However, the inside temperatures from the center and outwards can be approximated using these surfaces temperatures. The camera that will be used is the PYROVIEW 768N high-resolution IR camera from DIAS Infrared Systems [90]. It provides precise temperature measurements between 1673.15 and 3273.15 K (1400 - 3000 °C) - encompassing the expected combustion chamber temperature of 3030 K - with a frequency of 50 Hz, together with real-time video output in 768×576 pixel resolution through a Gigabit-Ethernet interface. The chosen model also has a protection housing made of stainless steel, with a protection window and water cooling possibility - which, if used, increases the maximum operating temperature from 50 to 150 °C.

4.3.6 Electrical interface

A complete electrical interfacing design, for the components connecting the propellant feed assembly components with the control station computer and its software, has not been developed as part of this thesis. However, in order to give an indication of what type of Input/Output (I/O) device will be needed, the selected components presented in the previous sections have been reviewed in order to determine their operation in terms of I/O signalling. The selected module will have to be able to

do Digital to Analog Conversion (DAC) for the control signals from the DCIS, as well as Analog to Digital Conversion (ADC) for the sensor signals to be read by the DCIS. Other electrical components and wiring will be needed to finish the design, however this preliminary review was done only to find a suitable main I/O module - partly in order to include an estimation for the electrical interfacing in the preliminary cost calculation.

As mentioned, the set point signals for the pressure regulator PID controllers will be delivered via USB to RS-232 communication directly from the control station. Also, the selected LC will deliver the measured thrust value through a 9 pin D-subminiature (D-sub) connector [79]. Thus, these two signals will not require any conversion and were not considered as part of the I/O signals for the I/O module. After reviewing the remaining components, it was determined that the SVs and the positioners for the RV actuators operate with analog signals and therefore require DAC. The sensor signals from the PSs, FMs and TSs (excluding TS2) are all analog and require ADC. In addition, PS5 and PS8 will require high impedance cables and charge amplifiers to convert the charge outputs to analog signals and the TSs will need transmitters to convert the small probe voltages to analog current signals. However, specific components for these parts have not been selected.

After counting the components it was determined that the I/O module must have at least eight analog outputs (3 RVs, 5 SVs) and 15 analog inputs (9 PSs, 3 FMs, 3 TSs). To fulfil this requirement, the selected component is the EtherTRAK-2 I/O Module from Red Lion [91] with 16 analog inputs and eight analog outputs.

4.4 Component costs

This section presents a table with summarised cost estimations relating to the hardware components of the propellant feed assembly. The table also includes an entry for the thrust chamber design related costs, although since the design is only preliminary at this point, the costs are unknown and listed with a To Be Determined (TBD) placeholder. Once a more refined design - with precise dimensions and shapes - has been developed in the future, the costs for thrust chamber materials, manufacturing etc. can be determined and added to the preliminary total cost.

Tab. 4.4 contains summarised costs for general hardware component types to give an idea of the costs for different categories. However, a more comprehensive table - with entries containing descriptions and unit prices of all specific components presented in this chapter - can be found in Tab. A.1 in Appendix A.

Not included in Tab. A.1 are the components of which specific units have not yet been selected. These are mostly components part of the physical design of the test platform structure - which has not yet been developed - or test environment components essential to the full integration and safe operation of all system parts; power supplies for the valves and sensors operating electronically, a water supply for thrust chamber cooling, a pressurised air supply for the gas pressure regulator valves and various other parts for the system framework structure - beams, fasteners, barricades etc. Furthermore, the length of tubing and number of tube unions required for the assembly are also unknown at this stage. Relating to the plumbing is also the selection of various adapter fittings that will be needed for whenever a component to be connected to a pipe has another size than the pipe it is to be connected to. These will be different depending on the connection type used by the component, e.g. flange, screw end, welded etc. All of these units will have to be selected by another project actor, in future iterations of design development leading up to the finalisation of the complete system design.

Other unselected components include the remaining parts of the ignition assembly - the switch, the capacitor and wiring - as well as a regular video camera used to monitor the thrust chamber during combustion tests. As mentioned previously, the design parameters of the fuel tank were given to

a professional pressure vessel manufacturing company - Tätsvets Hedqvist AB located in Tullinge, Sweden. The company then provided an estimation of the total cost for the drawing, manufacturing and control of the specified tank, which is presented in Tab. A.1.

The costs in Tab. A.1 have been grouped according to component categories, summed up and presented in Tab. 4.4.

TABLE 4.4: Summarised cost estimations of the hardware component categories. All costs in SEK. See Tab. A.1 for a comprehensive list of descriptions and prices for all specified components presented in Ch. 4.

Component category	Cost
Thrust chamber	TBD
Pressurised media supply tanks	106344
Flow control components: Valves, pressure regulators, filters, fuel injector, RD	410768
Parameter measurement components: Thrust, mass flow rate, pressure, temperature	526844
Ignition coil	135
I/O module	10710
PRELIMINARY TOTAL COST	1054801

Chapter 5

Software Design

5.1 Operations

This section describes the operations to be performed before, during and after a combustion test. The list of operations is used as a foundation for the design of the DCIS. The order of some operations are based on the ignition procedure presented in [15]. Operations are to be performed in the order shown below, starting with the system functionality test phase. See Fig. 4.4 for descriptions of components referred to in this section.

The following operations are assumed to have already been completed before the start of a new test:

- All plumbing has been emptied of residual propellants and purged with GN2. The GN2 has then been vented from the system.
- The fuel tank has been refilled.
- The GOx and GN2 supplies have been replenished.
- All valves have been closed.
- The consumed parts of the ignition assembly have been replaced and all parts of it have been assembled.

5.1.1 System functionality test phase

1. Perform a visual and thorough damage inspection on all propellant feed assembly components.
2. Turn on control and instrumentation system. Verify that all SVs, RVs and pressure regulator valves are in closed position. Verify that the FMs do not register any flow and that the pressure sensors register only ambient pressure (system not pressurised). Verify that temperature values are at expected levels.
3. Verify that all manual valves are closed. Check pressure gauges for additional verification that the system is not pressurised.
4. Open the regulator valve of the GOx pressure regulator assembly until fully open. Repeat for GN2 regulator assembly.
5. Open RV1 gradually until fully open. Repeat for RV2 and RV3. Open SV1. Verify that the FMs do not register any flow and that the pressure sensor read-outs show that pressure levels are unchanged (manual valves working and closed). Close SV1, all RV:s and both pressure regulator valves to fully closed.

6. For SV2, SV3, SV4 and SV5: Verify functionality of valves by opening and then closing each one in turn. Check pressure sensors again to verify expected pressure levels.
7. Test the ignition assembly and verify its functionality.

5.1.2 Combustion test preparation phase

8. Disconnect the ignition coil from its power supply.
9. Soak cotton on ignition assembly with gasoline. Insert and fasten the assembly in the combustion chamber.
10. Verify that SV3 is closed. Open manual valves MV1, MV2, MV3 and the valves of the GOx and GN2 supplies. Check that PG1 and PG4 display the cylinder pressure of $20 \cdot 10^6 \text{ Pa}$ (**200 bar**) and that PG2 and PG3 show no pressure level changes. Verify this by comparing with the read-outs of PS1 and PS9. Verify that the FMs do not register any flow.
11. Confirm that no GOx leaks are present by smelling the air surrounding the gas supply to try and detect the odour of the GOx supply additive.
12. Open SV5.
13. **Vacate all personnel from the test platform area.**

5.1.3 Combustion test phase

14. Set GN2 pressure regulator output pressure to the fuel tank operating pressure of $3.5 \cdot 10^6 \text{ Pa}$. Monitor the PS1 read-out until the operating pressure has been reached. Verify that SV1, SV2 and SV4 are closed and that the PS2, PS3 and PS9 pressure levels are unchanged.
15. Open SV1. Compare the pressure level outputs of PS1 and PS2 and verify equal pressure.
16. Set GOx pressure regulator output pressure to the oxidiser injector pressure of $2.534 \cdot 10^6 \text{ Pa}$ (this pressure level might have to be increased during the test, depending on pressure losses over RV3 and the resulting GOx mass flow rate). Monitor the PS9 read-out until the set pressure level has been reached.
17. Verify that the FMs do not register any flow (RVs working and closed).
18. Open RV2 gradually until the desired coolant water mass flow rate is registered by FM3. Verify that there are no leaks and that the water exits the thrust chamber via the outlet. Leave the water to flow through the chamber until the end of the combustion test, when the temperature has decreased to a safe level.
19. Reconnect the spark coil to its power supply.
20. Open RV3 slightly so that a small GOx flow can pass the ignition assembly. Close the ignition switch to energise the primary coil. Open the switch to create a spark which subsequently ignites the cotton. Verify the burning by monitoring the thrust chamber (through a camera).
21. Open RV1 slightly to introduce fuel into the combustion chamber. Verify that a flame appears at the nozzle exit.
22. Monitor the FM1, FM2 and PS5 read-outs as well as the thrust level output measured by the LC. Open RV1 and RV3 simultaneously to rapidly increase the propellant flow rates, until the desired values of combustion chamber pressure and fuel and oxidiser mass flow rates are reached.

If required, regulate the flow rates with RV1 and RV3 and the GOx pressure level with the GOx regulator, to control the thrust as displayed by the LC output. Also monitor TS2, TS3 and TS4 to verify that the combustion chamber does not get too hot and that the coolant water is absorbing a sufficient amount of heat.

23. End the combustion test. This can be done in three ways, through the ABORT procedure detailed in Sec. 5.1.4, or in one of the following ways:
 - If all fuel is to be used, let the combustion process end naturally. When the fuel has been consumed completely, the complete fuel section of the assembly will be automatically purged by the GN2 through the fuel tank, at which point the combustion will stop.
 - Alternatively, if the test is to be stopped before all fuel has been depleted, the operator must interrupt the process. First, stop the fuel flow by closing SV5. Then, open SV4 to purge the downstream fuel section with GN2.
24. Close GOx regulator valve to stop the GOx flow and open SV2 to purge the GOx section.
25. If there is residual fuel in the fuel tank and upstream feed line, extract it from the assembly through MV4 using a pump. When all fuel has been drained, close MV4 and open SV5 to completely purge the fuel section with GN2.
26. After purge completion, close the GN2 regulator valve. Vent the GN2 from the feed assembly by opening SV3.
27. Close all SVs, RV1 and RV3. After the combustion chamber temperature has decreased to a safe level, close RV2.
28. Close MV1, MV2 and MV3.
29. Vent the upstream regulator sections by opening MV5 and MV6 and then closing them again.

5.1.4 Combustion test ABORT procedure

Should the test have to be prematurely aborted - due to engine failure, over-pressurisation, excessive heat or other emergencies - the combustion must be abruptly stopped and the system stabilised. An ABORT button will be available in the DCIS. Pressing it will send signals to do the following simultaneously:

- **Close SV5 to stop the fuel flow.**
- **Close GOx regulator valve to stop the GOx flow.**
- **Open SV2 and SV4 to purge the remaining propellants from the feed lines with GN2.**

After this, the operations are continued from step 25 in Sec. 5.1.3.

5.2 Flowcharts of operations

The listed operations in the previous section have been summarised in flowchart format and displayed in Fig. 5.1 and Fig. 5.2. The former displays a flowchart of the overall test operations while the latter displays a flowchart of the system functionality test phase operations specifically, as described in Sec. 5.1.1.

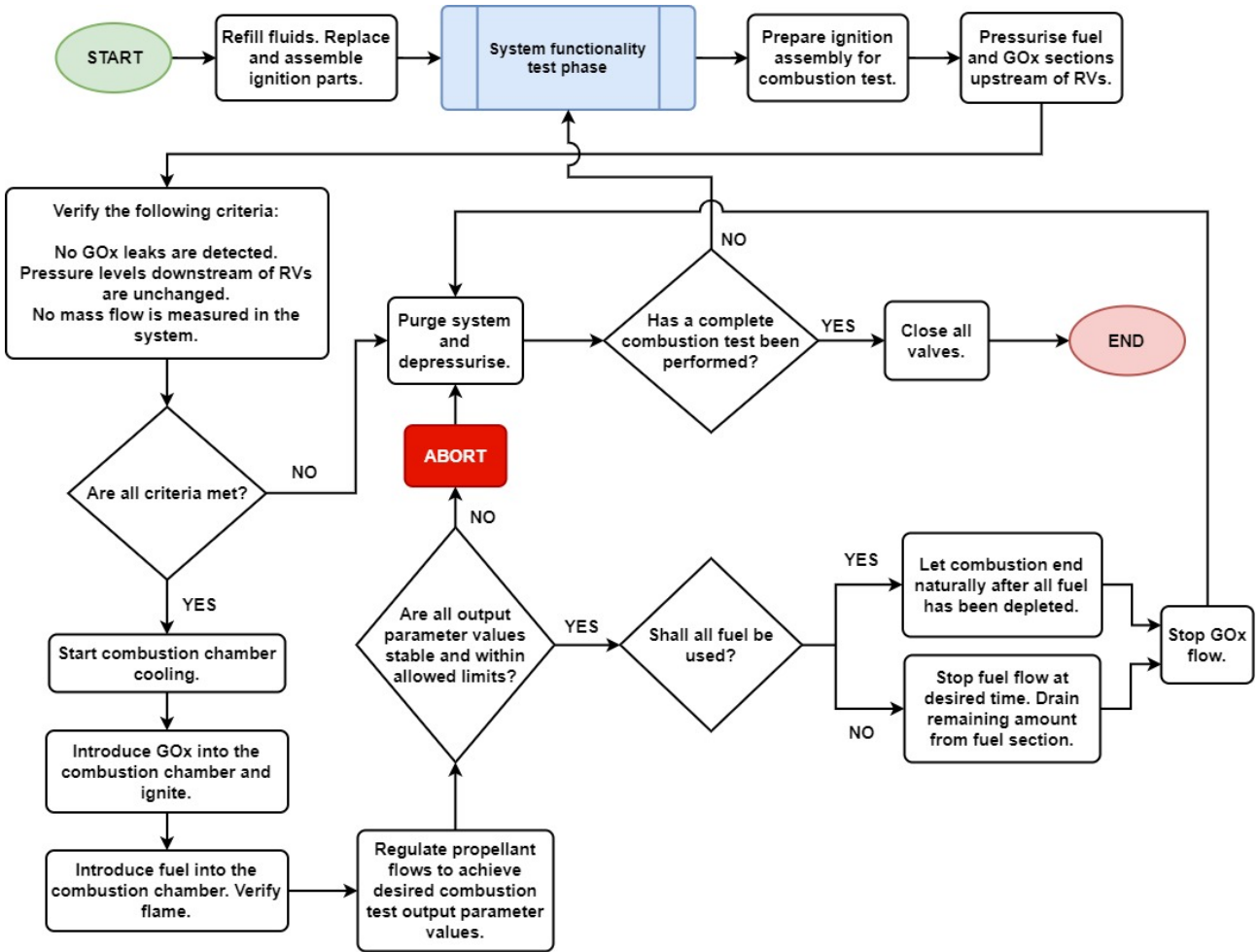


FIGURE 5.1: Flowchart summarising the operations to be performed before, during and after a combustion test. The operations of the system functionality test phase is represented here as a subroutine process and its contents are displayed in Fig. 5.2.

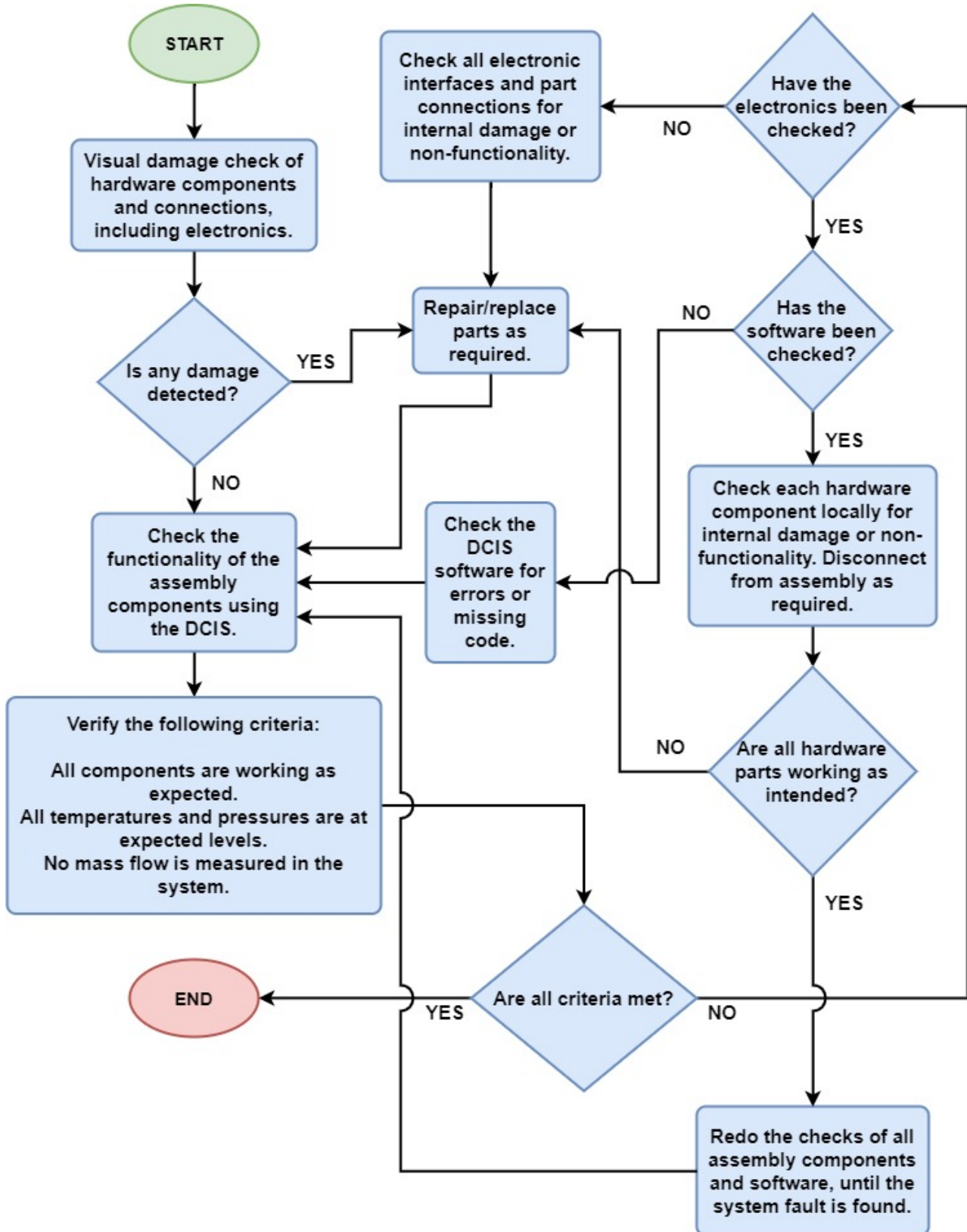


FIGURE 5.2: Flowchart summarising the operations of the system functionality test phase, shown as a subroutine process in Fig. 5.1.

5.3 Requirements

This section describes the functional requirements of the DCIS to be developed. The requirements are based partly on the Hardware Design section - describing which propulsion parameters that need to be measured, displayed and stored by the software - and partly on the list of operations, which gives an indication on how to group the different parts of the software system and what types of safety measures or other functions are needed at certain steps during the test phases. The list of operations is in this preliminary design not included as a software check list within the user interface. Currently, the list will have to be followed manually by the operator through the testing proceedings and he or she is trusted to go through the operations in the presented order - so that conducted tests are as safe as possible.

Some ideas on what is needed in this software are based on the developed software system in [34].

5.3.1 Data storage

Because the purpose of this system is not only to perform practical rocket propulsion tests, but also to compare obtained results with theoretically determined parameters, it is essential that the software has an option to store sensor data in addition to importing and displaying it to the operator in real time. The stored data can be used for various research purposes, for comparative studies of tests with varying input parameters and/or components or to calculate actual values of parameters that have either been assumed directly or calculated based on assumptions of system ideality. For example, the specific impulse of the system can be calculated with the integrals of measured thrust and total propellant mass flow over time and the WF exit velocity with average values of measured thrust chamber properties.

The sensor data will be stored in vectors in a folder specified by the operator and specific for the current test. The measured thrust data from the LC will, in addition, be stored as a graph over time which will be continuously updated and displayed to the operator during a test and then saved after combustion has stopped. The thrust chamber will be remotely monitored by two types of camera; one for regular video and one for IR temperature measurements of the chamber. The recordings of these camera outputs during combustion tests will also be stored in the same folder. The date of the test together with the test start time (the time when the operator instructs the DCIS to begin storing sensor data), the test end time (the time when the data storage is stopped), the ignition time and the combustion end time (the time when the operator sends a signal to the DCIS that the combustion has stopped) will all be saved in the selected folder as well.

5.3.2 User interface

As an aid in the work of the operator, the DCIS user interface will be organised in different sections - visualised in the program as screens - principally corresponding to the phases described in the operations list and the operations to be performed within them. This makes it so that during a certain test phase, the amount the operator has to switch between different screens is minimised. This is particularly important during the combustion test phase when many output parameters must be monitored concurrently and some input parameters are continuously varied. Common to all screens will be an output of the date and local time - continuously updated and displayed whenever the DCIS is turned on - as well as a visual alert signal. This signal will be activated on all screens if any measured pressure level and/or temperature within the propellant feed assembly should move to a value outside of its acceptable range set by the operator. Furthermore, the test start, test end, ignition and combustion end times will be displayed on all screens when triggered by the operator

throughout a test. A burn time timer will also be displayed on all screens, starting to count up at ignition and stopping at combustion end.

Configuration screen

This screen will be used for test configuration, that is it will allow the user to specify parameters pertaining to the test environment. For instance, on this screen the location for the data storage folder is specified and diagrams of the complete system are shown. This is also where the operator sets the acceptable parameter output ranges, which are referred to by the DCIS in order for it to make a decision whether to activate the visual alert signal.

Assembly overview screen

The assembly overview screen will have a diagram similar to the one shown in Fig. 4.4, where measured sensor values from each pressure sensor and temperature sensor probe will be displayed next to their respective sensor component within the diagram. Additionally, the diagram will contain state indicators next to each SV and the gas regulators - in the form of a light alternating between green and red - to indicate whether a valve is open or closed. Furthermore, the screen will have switches to allow the operator to either open or close the SVs and regulators. Most of the system functionality operations are performed via this screen.

This screen will also have an ACTIVE TEST switch which, when turned on, will instruct the DCIS to do the following:

- Display the time of test start on screen and store it in the specified data storage folder.
- Start the continuous storing of all measured sensor data, excluding the thrust data from the LC.
- Start the recording of the combustion chamber video and IR cameras.

The switch should be turned on just before the combustion test phase and turned off after the final operation of the phase. When turned off, the time of test end will be displayed on screen and stored, the sensor data storing will be stopped and the recordings of the cameras will be stopped and stored.

Combustion test screen

This screen will have all the controls and sensor outputs relating to the combustion test phase operations, up to and including the finalisation of the combustion process. Some of these will be duplicates of some of the assembly overview screen controls and outputs. This means, for example, that certain SVs can be actuated from either screen and their respective valve state indicators will at that point be updated simultaneously on both screens. Also, the sensors with two output displays will send their respective measurement signal concurrently to both screens, in order to update the values of both displays simultaneously. The reason for this, as mentioned previously, is to allow the operator to maintain focus on a single screen during the combustion phase of a test. Apart from convenience, this is also important from a safety standpoint as any errors or out-of-range parameter values can be detected and corrected faster. The contents of this screen will be divided into four main sections; a fuel section, a GOx section, a coolant water section and a thrust chamber section.

The fuel section will have an adjustment dial used to regulate the passage size through RV1, hence controlling the fuel flow, along with the same type of state indicator used for the SVs and gas regulators. It will also have an output display for the mass flow as measured by FM1. This type of

flow control setup will be used in the GOx and coolant water sections of the screen as well, using RV3/FM2 and RV2/FM3 respectively. Furthermore, the fuel section will have a switch to turn the GN2 regulator on and off, as well as a dial to set the outlet pressure with. It will also have output displays showing the resulting pressure levels in the GN2 and fuel feed assembly sections, as measured by PS1, PS2 and PS3. In addition, the section will have switches and state indicators for the SVs used to pressurise the fuel tank and closing off the downstream fuel section; SV1 and SV5, respectively.

The GOx section will, in addition to the flow control setup, have a switch and output pressure dial for the GOx regulator - the same type of setup as for the GN2 regulator. Also, this section will have output displays for the measured pressure levels of PS4 and PS9.

The coolant water section will have the aforementioned flow control setup as well as an output display showing the temperature of the water entering the combustion chamber coolant gap (TS4), the temperature of the water exiting it (TS3) and the difference between them (TS3 - TS4) - so that the operator can directly monitor how much heat from the combustion is absorbed during the process.

The combustion chamber section will display the thrust graph over time, getting input from the LC. It will also have output displays for the measured combustion chamber and nozzle exit pressure levels - getting input from PS5 and PS8 respectively. Additionally, this section will have an ENER-GISE and an IGNITE button. If the ignition assembly is connected to its power supply, pressing the former button will send a signal to close the ignition switch, in order to energise the primary coil, and pressing the latter button will send a signal to open the switch - generating a spark in the combustion chamber. If the ACTIVE TEST switch is turned on, pressing the IGNITE button will, in addition to generating a spark, instruct the DCIS to do the following:

- Display the time of ignition on screen and store it in the specified data storage folder.
- Start the continuous storing of the LC thrust data in vector format.
- Start sending the thrust data as input to the thrust graph display, for it to continuously update during the combustion process.
- Display the burn time timer on screen and start the count up.

The combustion chamber section will also have a COMBUSTION STOPPED button, which should be pressed by the operator as soon as the combustion is confirmed to have stopped - by monitoring both the combustion chamber camera and the thrust graph. When the button is pressed, the combustion end time will be displayed on screen and stored, the burn time timer will stop, the LC thrust data storing will stop, the DCIS will stop sending the thrust data to the thrust graph display and the final graph will be stored.

The combustion test screen will also have the ABORT button which will instruct the DCIS to start the procedure detailed in Sec. [5.1.4](#).

Additional screens

At least two additional screens will be part of the DCIS user interface, one for displaying the combustion chamber video camera output and one for the IR camera output. It will be important to have at least three physical monitors at the operator station, so that both of these camera outputs can be monitored in full-screen at the same time as the combustion test is controlled and monitored on a third screen.

Chapter 6

Discussion and conclusions

The objective of this thesis was to develop a preliminary design for a rocket engine testing platform and this has for all intents and purposes been achieved. A literature review was done in the beginning of the project to give an overview of all aspects of propulsion system types, their differences and hazards, parts included in their design and how they are controlled and tested. This review informed the decisions on the requirements for the hardware design, in terms of which type of propulsion and propellant combination to use for the platform as well as which materials to choose and which cooling method to implement, all with safety and simplicity in mind. There was an idea of some desired properties for the propulsion system to be designed at the start of the project, however the review turned out to be very helpful when actually deciding on the requirements. Particularly, it led to a better understanding of which propellants are the most hazardous and why and also helped guide the overall design based on required components for these types of systems.

6.1 Thrust chamber

Using the requirements as well as research done for the selected propellant combination as a foundation, a thrust chamber design was developed. Some parameter values were used directly from various sources based on recommendations but most were calculated using equations based on assumptions of system ideality. The result is a small, water-cooled thrust chamber made of copper, theoretically capable of delivering 1000 N of thrust using GOx as oxidiser and a 70 % concentrated ethanol-water mixture as fuel.

The value of the annular coolant water flow gap, between the outer surface of the thrust chamber and the inner surface of the cooling jacket, was calculated to approximately 0.05 mm. This value seems very small, especially compared to the calculated value for a similar sized rocket engine presented in [15]: 1.0795 mm (0.0425 in). The calculations done for the design presented in Ch. 4 have been checked but no error has been found. As part of the continuation of this project they might have to be checked again, however if confirmed to be correct, the gap might still have to be increased - if deemed to be impractical from a manufacturing standpoint. Another option would be to consider another cooling method, such as ablative cooling.

6.2 Propellant feed assembly

Based in the literature review and using other test platform designs as reference, a design of a complete propellant feed assembly with all required components was developed as part of the propulsion system hardware design. The assembly uses the gas pressure feed technique, utilising a supply of pressurised GN2 to feed the fuel mixture from its tank towards the thrust chamber for combustion.

Also included in the assembly are various types of valves, sensors and other components - all necessary for optimal and safe rocket engine operation and testing. As it turned out, the design of the propellant feed assembly - including the research made for deciding on specific components to use - took longer than was initially expected. The work was not straightforward and the design went through several iterations as new required system functions were recognised. Moreover, component parts were added and others were replaced throughout the design process, in order to fulfil all specifications and to make sure that all selected parts were compatible with each other. To give an idea of this process, the schematic diagram shown in Fig. 4.4 is the 11th version of the original design.

6.3 Costs

Also as part of the hardware design section, the costs for all selected hardware components were determined and summarised with part descriptions in a component cost table. For the components selected as part of this thesis, the total estimated cost is **1054801 SEK**.

6.4 Software

Furthermore, an operations list was produced, including all operations needed to be performed before, during and after a combustion test. A specific abort procedure for combustion testing, to be followed in case of emergencies, was developed as well. The operations were summarised in flowcharts which give an overview of the combustion testing procedure and can be followed when operating the finished platform. The listed operations, together with described propulsion system parameters, were used to develop the DCIS software design, presented in text as software requirements. The requirements section explains all necessary parts of the software; how it should operate in terms of data collection and storage and how it should be visualised in terms of its user interface. Unfortunately, due to time constraints, the software could not be implemented in a program such as LabVIEW, nor could it be tested with simulated propulsion system parameters.

6.5 Encountered problems and design changes

6.5.1 Changes to propellant feed assembly structure

As mentioned, changes were made to the design of the propellant feed assembly structure throughout the design process. This happened whenever it was realised that the system would require some function that had not previously been considered or, contrarily, that some existing function(s) were not necessary for the system operation. Many of the changes were made after discussing with and getting input from Olle Persson and the project supervisor. For example, the upstream sections of the pressure regulators each initially had one SV and one MV, to control the gas flows between the supplies and the regulator valves. This was later deemed to be redundant, as the gas cylinders come with manual valves included and the remote control of the regulator valve will be sufficient without the need to remotely control the incoming gas flow with a SV as well. Another example is that the GN2 section connected to the GOx section via SV2, for flushing purposes, was not included initially, as the fact that the GOx section would need to be flushed after a test had not been considered at first.

6.5.2 Component changes

When first selecting the SVs, whether they were of the normally closed or normally open type was not realised to be of importance and the valves were selected with no thought of this. However, later in the process it was realised that if there is a power outage it will be important that SV5 remains open while the other SVs are closed, as a safety feature. Because of this, the SV selection was revised with their normal state in mind.

Initially, each pressure regulator assembly consisted of only one regulator component, specifically the EPR 3000 high precision electronic pressure regulator, capable of delivering an outlet pressure between 0 and $20.7 \cdot 10^6$ Pa (3000 psi) for a maximum inlet pressure of $23.79 \cdot 10^6$ Pa (3450 psi) or 237.9 bar. Pressure measurement, control signal calculation and valve actuation is all done internal to the regulator. Also, the first selected component for the FMs was the Proline Promass F 300 stainless steel Coriolis flowmeter from Endress+Hauser, rated for $4 \cdot 10^6$ Pa (40 bar) and capable of measuring liquid mass flows up to 0.56 kg s^{-1} and gaseous mass flows up to 0.31 kg s^{-1} , according to calculations done based on data sheet information. Both of these components were selected because it seemed that they fulfilled the specifications, in terms of pressures and required flow rates. However, after discussing their properties and application with distributor representatives from their respective suppliers, it was discovered that the flow rates through the system would be much more than the components could handle - something that was overlooked during the initial selection. Fortunately, with suggestions from the distributor representatives, new solutions could be found for these components.

6.6 Future work

6.6.1 Finalisation of testing platform

For this master thesis, a preliminary design of a rocket engine testing platform has been developed. However, the goal of the project that has now been initialised is of course to finalise the design of the platform and eventually construct it, for it to be used as intended. To get to that point, there are several things that need to be done.

Software tasks

The DCIS software needs to be finalised. That is, the design presented in this report should be implemented through programming by integrating with an application developing program, e.g. LabVIEW. Software simulations with simulated parameters should then be performed, in order to verify that the finished software works as intended. If using LabVIEW, setting up virtual drivers to represent different hardware components can be useful for this purpose.

Hardware tasks

The finalisation of the hardware design has three parts. First, the propellant feed assembly design needs to be finalised in terms of component selection. There are still some components that have not been selected, and the already selected ones should be reviewed in order to verify their compatibility within the application and, if needed, to replace components if more suitable or less expensive ones are found. Also, a physical design for the complete platform needs to be developed - that is a plan that shows how the different components of the assembly are to be mounted in relation to each other

within the actual platform and also in relation to the operator's station, according to standards and regulations, to guarantee the safety of the personnel.

Secondly, the preliminary thrust chamber design should be reviewed, after which a more detailed 3-dimensional model should be developed. When such a model has been produced, different types of simulations can be performed on it, to determine performance properties. These simulations can include structural and thermal analyses as well as combustion simulations, using the calculated injection pressures and mass flows and with the selected propellants. The last step would be to manufacture and assemble the thrust chamber within the remaining propellant feed assembly.

Finally, the electrical interfacing between the hardware components and the software, e.g. ADC and DAC or other types of signal processing, needs to be designed and implemented.

6.6.2 Improvements and future developments of finished platform

Once the platform has been finished, some plans for future potential improvements, or further developments, have been discussed. The control of mass flow rates during a combustion test could be automated by implementing PID controllers, connected between the FMs and RVs and receiving set point signals from the DCIS - similarly to how the pressure is regulated in the pressure regulator assemblies.

Another future development could be to re-design the thrust chamber nozzle to be segmented horizontally, so that segments can be removed or added in order to practically test the influence of ϵ on thrust generation. This type of nozzle design can be seen in [34].

The presented design could also work with a hybrid type propellant rocket engine. While still using GOx as oxidiser, the ethanol-water liquid fuel could be replaced with a solid propellant - stable and safe enough to be used within this application.

References

- [1] Deutsches Zentrum für Luft- und Raumfahrt, *DLR Lampoldshausen*. [Online]. Available: <https://www.dlr.de/content/en/articles/sites/lampoldshausen/about-lampoldshausen.html> (Accessed: 29/11/2019).
- [2] P. Smith, *Skyrora opens secret rocket engine testing facility*, Oct. 2019. [Online]. Available: <https://www.aerospacetestinginternational.com/news/engine-testing/skyrora-opens-secret-rocket-engine-testing-facility.html> (Accessed: 29/11/2019).
- [3] Swedish Space Corporation, *ESRANGE SPACE CENTER - Europe's largest civilian space center*. [Online]. Available: <https://www.sscspace.com/ssc-worldwide/esrange-space-center/> (Accessed: 02/12/2019).
- [4] Swedish Space Corporation, *ESRANGE TESTBED - Excellent test facilities for your specific needs*. [Online]. Available: <https://www.sscspace.com/services/science-and-launch-services/testbed/> (Accessed: 02/12/2019).
- [5] Swedish Space Corporation, *SSC and DLR to strengthen Europe's capacity for rocket development*, Oct. 2019. [Online]. Available: <https://www.sscspace.com/ssc-dlr-strengthen-europe-capacity-rocket-development/> (Accessed: 02/12/2019).
- [6] European Cooperation for Space Standardization, *Space project management - project planning and implementation*, ECSS-M-ST-10C. Rev. 1, Mar. 2009.
- [7] Goodreads, Inc, *Rocket Propulsion Elements*, 2019. [Online]. Available: <https://www.goodreads.com/book/show/7682536-rocket-propulsion-elements> (Accessed: 28/11/2019).
- [8] G. P. Sutton and O. Biblarz, *Rocket Propulsion Elements*, 9th ed. NJ, USA: John Wiley & Sons, Inc., 2017.
- [9] Amazon.com, Inc, *HOW to DESIGN, BUILD and TEST SMALL LIQUID-FUEL ROCKET ENGINES*. [Online]. Available: <https://www.amazon.com/DESIGN-BUILD-LIQUID-FUEL-ROCKET-ENGINES/dp/B005D3P30Q> (Accessed: 28/11/2019).
- [10] NASA, *Rocket parts*. 2014. [Online]. Available: <https://www.grc.nasa.gov/WWW/K-12/rocket/rockpart.html> (Accessed: 26/04/2019).
- [11] R. W. Buchheim, *SPACE HANDBOOK: ASTRONAUTICS AND ITS APPLICATIONS*. NY, USA: Random House, 1959.
- [12] NASA, *Rocket thrust*. 2014. [Online]. Available: <https://www.grc.nasa.gov/WWW/K-12/rocket/rktth1.html> (Accessed: 26/04/2019).
- [13] P. Berlin, *Satellite Platform Design*, 6th ed. Kiruna, Sweden: Luleå University of Technology, 2014.
- [14] NASA Glenn Research Center, *Magnetoplasmadynamic thrusters*. Nov. 2004. [Online]. Available: <https://www.nasa.gov/centers/glenn/about/fs22grc.html> (Accessed: 14/05/2019).

- [15] L. J. Krzycki, *HOW to DESIGN, BUILD and TEST SMALL LIQUID-FUEL ROCKET ENGINES*. CA, USA: Rocketlab, 1967.
- [16] *Safety Data Sheet - Material Name: Gasoline All Grades*, SDS No. 9950, Hess Corporation, Aug. 2012.
- [17] *MATERIALS SAFETY DATA SHEET (MSDS) Ethanol (C₂H₅OH)*, MSDS Number NCP/P/1, NCP Alcohols, Aug. 2018.
- [18] *Safety Data Sheet - Material Name: Kerosene K1 and K2*, SDS No. 0290, Hess Corporation, Aug. 2012.
- [19] Canadian Centre for Occupational Health and Safety, *OSH Answers Fact Sheets - Gasoline*. [Online]. Available: https://www.ccohs.ca/oshanswers/chemicals/chem_profiles/gasoline.html (Accessed: 26/10/2019).
- [20] Crown Oil Ltd, *Guide to Kerosene*, 2019. [Online]. Available: <https://www.crownoil.co.uk/guides/kerosene-guide/> (Accessed: 26/10/2019).
- [21] CAMEO Chemicals, *GASOLINE*. [Online]. Available: <https://cameochemicals.noaa.gov/chemical/11498> (Accessed: 26/10/2019).
- [22] CAMEO Chemicals, *ETHANOL*. [Online]. Available: <https://cameochemicals.noaa.gov/chemical/667> (Accessed: 26/10/2019).
- [23] CAMEO Chemicals, *KEROSENE*. [Online]. Available: <https://cameochemicals.noaa.gov/chemical/960> (Accessed: 26/10/2019).
- [24] CAMEO Chemicals, *JET FUELS, [JP-5]*. [Online]. Available: <https://cameochemicals.noaa.gov/chemical/11699> (Accessed: 26/10/2019).
- [25] *Safety Data Sheet - Material Name: Jet Fuel JP5*, SDS No. 9942, Hess Corporation, Aug. 2012.
- [26] CAMEO Chemicals, *METHANE, REFRIGERATED LIQUID (CRYOGENIC LIQUID)*. [Online]. Available: <https://cameochemicals.noaa.gov/chemical/3872> (Accessed: 26/10/2019).
- [27] *Methane Safety Data Sheet*, SDS No. 8010, Rev. date: 30/10/2018, Hess Corporation, Nov. 2015.
- [28] Canadian Centre for Occupational Health and Safety, *OSH Answers Fact Sheets - Methane*. [Online]. Available: https://www.ccohs.ca/oshanswers/chemicals/chem_profiles/methane.html (Accessed: 26/10/2019).
- [29] Matheson Tri-Gas, Inc, *Materials Compatibility Guide*. [Online]. Available: <https://www.mathesongas.com/pdfs/products/Materials-Compatibility-Guide.pdf> (Accessed: 27/10/2019).
- [30] NASA, *Rocket thrust equations*. 2014. [Online]. Available: <https://www.grc.nasa.gov/WWW/K-12/rocket/rktthsum.html> (Accessed: 26/04/2019).
- [31] NASA, *Compressible area ratio*. 2014. [Online]. Available: <https://www.grc.nasa.gov/WWW/K-12/rocket/astar.html> (Accessed: 29/04/2019).
- [32] NASA, *Nozzle design*. 2014. [Online]. Available: <https://www.grc.nasa.gov/WWW/K-12/rocket/nozzle.html> (Accessed: 29/04/2019).
- [33] Smithsonian National Air and Space Museum, *Cooling Jacket, Water, Rocket Motor, Goddard, Half*. [Online]. Available: <https://airandspace.si.edu/collection-objects/cooling-jacket-water-rocket-motor-goddard-half> (Accessed: 29/10/2019).

- [34] E. Santos, W. Alves, A. Prado and C. Martins, 'Development of test stand for experimental investigation of chemical and physical phenomena in liquid rocket engine', *Journal of Aerospace Technology and Management*, vol. 3, no. 2, pp. 159–170, Aug. 2011.
- [35] Microsoft, *What is .NET Framework?*, 2019. [Online]. Available: <https://dotnet.microsoft.com/learn/dotnet/what-is-dotnet-framework> (Accessed: 03/11/2019).
- [36] S. H. Pavuluri, 'Development of an Automated Test Platform for Characterization and Performance Assessment of Electronic Modules in Electric Thrusters: The TESPEMET Project', Master's Thesis, Luleå tekniska universitet, Oct. 2019.
- [37] Electronics Notes, *What is LabVIEW?* [Online]. Available: <https://www.electronics-notes.com/articles/test-methods/labview/what-is-labview.php> (Accessed: 30/07/2019).
- [38] National Instruments, *What Is LabVIEW?*, 2019. [Online]. Available: <https://www.ni.com/service/shop/labview.html> (Accessed: 30/07/2019).
- [39] Engineering ToolBox, *Altitude above sea level and air pressure*, 2003. [Online]. Available: https://www.engineeringtoolbox.com/air-altitude-pressure-d_462.html (Accessed: 24/06/2019).
- [40] T. Helmenstine, *How to calculate the density of a gas*, 2018. [Online]. Available: <https://www.thoughtco.com/calculate-density-of-a-gas-607553> (Accessed: 26/06/2019).
- [41] D. Almeida and C. Pagliuco, 'Development status of l75: A brazilian liquid propellant rocket engine', *Journal of Aerospace Technology and Management*, vol. 6, no. 4, pp. 475–484, Dec. 2014.
- [42] Sandmeyer Steel Company, *Stainless steel plate alloy 316/316l*, 2016. [Online]. Available: <https://www.sandmeyersteel.com/316-316L.html#GeneralProperties> (Accessed: 04/07/2019).
- [43] C. Gottman, W. Alves, J. Rocco, K. Iha and R. Goncalves, 'Liquid rocket propellants: Ethanol as fuel', *GLOBAL JOURNAL OF ADVANCED RESEARCH*, vol. 2, no. 1, pp. 109–119, Jan. 2015.
- [44] D. P. Rowlands, 'The mechanical properties of stainless steel', Southern Africa Stainless Steel Development Association, Tech. Rep. STAINLESS STEEL INFORMATION SERIES NO. 3.
- [45] C. Nordling and J. Österman, *Physics Handbook for Science and Engineering*, 8th ed. Poland: Dymograf, 2014.
- [46] AppliChem GmbH, *Ethanol 70 % (dab) pure, pharma grade*, 2019. [Online]. Available: <https://www.applichem.com/en/shop/product-detail/as/ethanol-70-reinst-dab/> (Accessed: 05/07/2019).
- [47] McMaster-Carr Supply Company, *Full-Cone Spray Nozzle*. [Online]. Available: <https://www.mcmaster.com/32885k151> (Accessed: 06/11/2019).
- [48] Engineering ToolBox, *Gases - densities*, 2003. [Online]. Available: https://www.engineeringtoolbox.com/gas-density-d_158.html (Accessed: 05/07/2019).
- [49] National High Magnetic Field Laboratory, *INTERACTIVE TUTORIALS - Ignition Coil*. [Online]. Available: <https://nationalmaglab.org/education/magnet-academy/watch-play/interactive/ignition-coil> (Accessed: 24/09/2019).
- [50] Biltema, *IGNITION COIL*. [Online]. Available: <https://www.biltema.se/en-se/car---mc/car-spares/ignition-parts/ignition-coils/ignition-coil-2000037038> (Accessed: 09/08/2019).
- [51] Edrawsoft, *Standard P&ID Symbol Legend | Industry Standardized P&ID Symbols*, 2019. [Online]. Available: <https://www.edrawsoft.com/pid-legend.php> (Accessed: 03/11/2019).

- [67] *Stainless Steel High Pressure Relief Valve (Liquid & Gas)*, RVC-05-Npt Product specifications, Stra-Val, 2019.
- [68] R. King, J. Lindberg and M. Tornblad, *RE: Help with burst disk selection*, Personal emails, Aug. 2019.
- [69] *Offert för ZOOK Sprängbleck*, Component quotation 819035, PROCAB AB, Aug. 2019.
- [70] *PB Series Forward-Acting Metal Rupture Disks*, PB Series Datasheet, ZOOK Enterprises LLC, Feb. 2019.
- [71] *Screw Type Disk Holders*, Screw-Type Datasheet, ZOOK Enterprises LLC, Jan. 2018.
- [72] *High Pressure and Severe Service Valve - Type 1711*, RCV-DS-00578-EN-03 Datasheet, Badger Meter, Inc., Aug. 2015.
- [73] N. Gilbert (AZoNetwork), *Stellite Alloys - Chemical Composition, Mechanical Properties and Common Applications*, 2013. [Online]. Available: <https://www.azom.com/article.aspx?ArticleID=9857> (Accessed: 01/11/2019).
- [74] A. Bergsma (Pressure Control Solutions), *RE: Quotation pressure regulator*, Personal emails (regulator valve sizing calculations), Oct. 2019.
- [75] *Actuator Assembly - Type PA35 Multi-Spring Pneumatic Actuator*, RCV-DS-00618-EN-03 Data- sheet, Badger Meter, Inc., Aug. 2015.
- [76] *TK PRESSURE TRANSMITTER*, DTS_TK_05-2016_ENG Datasheet, GEFRAN, May 2016.
- [77] A. Bergsma, *Quotation 201910000086*, Oct. 2019.
- [78] McMaster-Carr Supply Company, *High-Pressure Inline Filter*. [Online]. Available: <https://www.mcmaster.com/9811k86> (Accessed: 13/08/2019).
- [79] *Strain Gage Load Cell*, 4578A Datasheet, Kistler Group, Sep. 2011.
- [80] *Proline Promass F 300 - Coriolis flowmeter*, TI01221D Technical information, Endress+Hauser, Jul. 2019.
- [81] H. Berts (Endress+Hauser), *RE: Offert flödesmätare*, Personal emails (flowmeter sizing calculations), Oct. 2019.
- [82] AMETEK Inc., *ALLOY C22 · UNS N06022*, 2018. [Online]. Available: <https://www.finetubes.co.uk/products/materials/nickel-alloy-tubes/alloy-c22-uns-n06022> (Accessed: 31/10/2019).
- [83] *Proline Promag H 300 - Electromagnetic flowmeter*, TI01223D Technical information, Endress+Hauser, Jul. 2019.
- [84] *Pressure gauge - stainless steel degreased for oxygen*, E 02.08.05 Datasheet, AB Svenska Industri Instrument SINI, Jan. 2017.
- [85] ENGINEERED SOFTWARE, INC., *Understanding the Distinction Between Total, Static and Dynamic Pressure*, 2017. [Online]. Available: <https://eng-software.com/about-us/press/articles/understanding-the-distinction-between-total-static-and-dynamic-pressure/> (Accessed: 18/10/2019).
- [86] *Piezoelectric pressure sensor Type 603C*, 603C_003 – 288e – 03.19 Datasheet, Kistler Group, Mar. 2019.
- [87] *Instruction Manual, Piezoelectric Pressure Sensors Type 601C Type 603C*, 60xx_002 – 741e – 03.19 Manual, Kistler Group, Mar. 2019.

- [88] *M6 absolute pressure transmitter Type 4080B*, 4080B_003 – 415e – 12.18 Datasheet, Kistler Group, Dec. 2018.
- [89] MincoComponents, *Immersion RTDs: S604PD40Z120T*. [Online]. Available: http://catalog.minco.com/catalog3/d/minco/?c=products&cid=1_6_4-immersion-rtds&id=S604PD40Z120T (Accessed: 13/08/2019).
- [90] PYROVIEW 768N, Datasheet, DIAS Infrared GmbH, Apr. 2018.
- [91] Red Lion, *ETHERTRAK-2 I/O MODULE-16 ANALOG INPUTS/8 ANALOG OUTPUTS*, 2019. [Online]. Available: <https://www.redlion.net/product/ethertrak-2-io-module-16-analog-inputs8-analog-outputs> (Accessed: 07/11/2019).

Appendix A

Component cost table

Below is a table containing estimated costs for all selected hardware components presented in Ch. 4. The unit prices listed in Tab. A.1 have been sourced either directly from the supplier website or from quotations through email, prepared by representatives of either the supplier or of one of their distributors. The currency of all listed prices is SEK. In the cases when the prices have been given in other currencies, namely EUR and USD, the following rates have been applied for the conversion: 1 USD = 9.64 SEK, 1 EUR = 10.73 SEK. All unit prices have been rounded up to the nearest whole number. Tax and shipping costs are not included in the prices.

TABLE A.1: Component cost estimations. All costs in SEK. Refer to Ch. 4 for component descriptions. Components listed in the order of appearance in the text.

Component(s)	Supplier	Unit description	Unit price	Quantity	Cost
Thrust chamber	TBD	Combustion chamber and de Laval nozzle, copper, machined as one piece, $L_c = 90.5$ mm, $L_{con} = 14.43$ mm, $L_{div} = 34.49$ mm, $D_c = 74.96$ mm, $D_t = 24.99$ mm, $D_e = 43.47$ mm, $t_{cw} = 4.08$ mm, $\alpha = 15^\circ$, $\beta = 60^\circ$. Four GOx injector holes, $D_{inj} = 3.72$ mm. Cooling jacket, austenitic stainless steel type SAE 316L, $t_{jw} = 0.78$ mm, $d_{gap} = 0.05$ mm.	TBD	1PC	TBD
Fuel injector	McMaster-Carr	Full-Cone Spray Nozzle, type 32885K151, 120° spray angle, 16.65 L min ⁻¹ volume flow rate, brass, 1/4" National Pipe Thread (NPT) screw end connection.	116	1PC	116
Ignition coil	Biltema	12 V Ignition Coil, article 53-400, oil-filled and oil-cooled.	135	1PC	135
Fuel tank	Tätsvets Hedqvist AB	Fuel tank 20 L, stainless steel, $7 \cdot 10^6$ Pa design pressure, one inlet and two outlets. Including construction drawing, construction control, manufacturing of the tank and manufacturing control.	103900	1PC	103900

Continued on next page.

Table A.1 – continued from previous page.

Component(s)	Supplier	Selected unit	Unit price	Quantity	Cost
GOx supply	AGA	ODOROX® cylinder, part 102785, 50 L, 200 bar, odorised.	974	2PC	1948
GN2 supply	AGA	Nitrogen cylinder, part 100258, 20 L, 200 bar.	496	1PC	496
SV5	ASCO	Series 262 direct acting 2 way solenoid valve, type 8262H080, stainless steel, normally closed, 1/4" NPT screw end connections, $5.17 \cdot 10^6$ Pa pressure rating.	1061	1PC	1061
SV1, SV2, SV3, SV4	ASCO	Series 262 direct acting 2 way solenoid valve, type 8262H130, stainless steel, normally open, 1/4" NPT screw end connections, $4.48 \cdot 10^6$ Pa pressure rating.	2391	4PC	9564
MV1, MV2, MV3, MV4	Flowserve Worcester Controls	Series 59 Full-Port Ball Valve, stainless steel, TFE seat, 1/4" NPT screw end connections, $6.9 \cdot 10^6$ Pa pressure rating.	3970	4PC	15880
MV5	Swagelok	SK Series multipurpose ball valve, part SS-4SKPF4, stainless steel, PEEK seats, 1/4" NPT screw end connections, 413 bar pressure rating.	2702	1PC	2702
MV6	Swagelok	SK Series multipurpose ball valve, part SS-4SKPS6, stainless steel, PEEK seats, 3/8" Swagelok tube fittings, 413 bar pressure rating.	2906	1PC	2906
CV1, CV3, CV4	Swagelok	CP Series 1-Piece Poppet Check Valve, part SS-4CP2-1, stainless steel, 1/4" NPT screw end connections, $20.6 \cdot 10^6$ Pa pressure rating.	392	3PC	1176
CV2, CV5	Swagelok	CP Series 1-Piece Poppet Check Valve, part SS-8CP2-1, stainless steel, 1/2" NPT screw end connections, $20.6 \cdot 10^6$ Pa pressure rating.	955	2PC	1910

Continued on next page.

Table A.1 – continued from previous page.

Component(s)	Supplier	Selected unit	Unit price	Quantity	Cost
RV2 assembly	Flowserve Worcester Controls	CPT Characterized Seat Control Valve, model CPT44, three-piece configuration, stainless steel, "Metal A" seat, 1/4" NPT screw end connections, $9.8 \cdot 10^6$ Pa pressure rating. Series 75 Electric Actuator, size 10, 100% duty cycle, 120 VAC at 50 Hz, TYPE 1 General Purpose enclosure. Including an actuator mounting kit and a DFP17 DataFlo P™ positioner, with 4 - 20 mA input, 4 - 20 mA position feedback, 120 VAC at 50 Hz.	61800	1PC	61800
RV1 assembly	Flowserve Worcester Controls	CPT Characterized Seat Control Valve, model CPT94, three-piece configuration, stainless steel, "Metal A" seat, 1/4" NPT screw end connections, $9.8 \cdot 10^6$ Pa pressure rating. Series 75 Electric Actuator, size 12, 100% duty cycle, 120 VAC at 50 Hz, TYPE 1 General Purpose enclosure. Including an actuator mounting kit and a DFP17 DataFlo P™ positioner, with 4 - 20 mA input, 4 - 20 mA position feedback, 120 VAC at 50 Hz.	65795	1PC	65795
RV3 assembly	Flowserve Worcester Controls	CPT Characterized Seat Control Valve, model CPT94, three-piece configuration, stainless steel, "Metal A" seat, 1/2" NPT screw end connections, cleaned for GOx use, $9.8 \cdot 10^6$ Pa pressure rating. Series 75 Electric Actuator, size 12, 100% duty cycle, 120 VAC at 50 Hz, TYPE 1 General Purpose enclosure. Including an actuator mounting kit and a DFP17 DataFlo P™ positioner, with 4 - 20 mA input, 4 - 20 mA position feedback, 120 VAC at 50 Hz.	66895	1PC	66895
PRV1	Straval	High Pressure Relief Valve, model RVC05-02T, stainless steel, PTFE seat, 1/4" NPT screw end connections, $10.34 \cdot 10^6$ Pa pressure rating, $0.86 \cdot 10^6$ - $7.58 \cdot 10^6$ Pa set relief pressure range.	4637	1PC	4637

Continued on next page.

Table A.1 – continued from previous page.

Component(s)	Supplier	Selected unit	Unit price	Quantity	Cost
PRV2	Straval	High Pressure Relief Valve, model RVC05-03T, stainless steel, PTFE seat, 3/8" NPT screw end connections, $10.34 \cdot 10^6$ Pa pressure rating, $1.03 \cdot 10^6$ - $8.62 \cdot 10^6$ Pa set relief pressure range.	4753	1PC	4753
RD	ZOOK	Pre-Bulged Forward-acting type Disc (PB-ST), size 1/2", stainless steel, fits 30° angle-seated ST disk holder, $7 \cdot 10^6 \pm 10\%$ Pa burst pressure.	1120	1PC	1120
RD holder	ZOOK	Screw Type 30° Angle Seated Holder (ST), stainless steel, 1/2" NPT screw end inlet connection.	3685	1PC	3685
GOx pressure regulator assembly	Badger Meter RCV	High Pressure and Severe Service Valve, equal percentage normally closed globe control valve type 1711, $34.5 \cdot 10^6$ Pa pressure rating, 0.07 - 0.26 kg s^{-1} mass flow rate operating range, stainless steel/stellite, cleaned for GOx use, size DN25, 1" NPT screw end connections. Multi-Spring Pneumatic Actuator, ATO type PA35, $4 \cdot 10^5$ Pa pressure rating, stainless steel, 0.2 - 1 bar control pressure. Including a 4 - 20 mA to 0.2 - 1 bar I/P transducer and an air filter regulator.	71140	1PC	71140
GN2 pressure regulator assembly	Badger Meter RCV	High Pressure and Severe Service Valve, equal percentage normally closed globe control valve type 1711, $34.5 \cdot 10^6$ Pa pressure rating, 0.04 - 0.2 kg s^{-1} mass flow rate operating range, stainless steel/stellite, size DN25, 1" NPT screw end connections. Multi-Spring Pneumatic Actuator, ATO type PA35, $4 \cdot 10^5$ Pa pressure rating, stainless steel, 0.2 - 1 bar control pressure. Including a 4 - 20 mA to 0.2 - 1 bar I/P transducer and an air filter regulator.	65228	1PC	65228
Regulator pressure transmitter	GEFRAN	Pressure Transmitter, type TK-E-1-Z-B04D -M-V, 0 - $4 \cdot 10^6$ Pa measuring range, $8 \cdot 10^6$ Pa pressure rating, stainless steel alloys. Including a 4 pin to SubD9 Male/Female adapter for PID controller connection.	3101	2PC	6202

Continued on next page.

Table A.1 – continued from previous page.

Component(s)	Supplier	Selected unit	Unit price	Quantity	Cost
Regulator PID controller	Pressure Control Solutions	PID Controller, model PCS-PID-AGD, 4 - 20 mA set point input signal (via RS-232), 4 - 20 mA remote pressure transmitter input signal, 4 - 20 mA control output signal. Including USB to RS-232 converter for PC connection, RS-232 cabling and a power adapter.	11192	2PC	22384
F1, F2	McMaster-Carr	High-Pressure Inline Filter, part 9811K86, stainless steel, 10 micron particle filtering, 1/4" NPT screw end connections, 20.7 · 10^6 Pa pressure rating.	907	2PC	1814
LC	Kistler	Strain Gage Load Cell, type 4578A10C3, 0 - 10^4 N measuring range, stainless steel.	9450	1PC	9450
FM1	Endress+Hauser	Coriolis flowmeter, Proline Promass F300 model, $10 \cdot 10^6$ Pa pressure rating, 0 - 1.806 kg s^{-1} mass flow rate operating range, stainless steel, size DN15, PN100 EN1092-1-B2 standard raised face flange connections.	73500	1PC	73500
FM2	Endress+Hauser	Coriolis flowmeter, Proline Promass F300 model, $10 \cdot 10^6$ Pa pressure rating, 0 - 1.092 kg s^{-1} mass flow rate operating range, Alloy C22, cleaned for GOx use, size DN15, PN100 EN1092-1-D standard grooved flange connections.	110000	1PC	110000
FM3	Endress+Hauser	Electromagnetic flowmeter, Proline Promag H300 model, $4 \cdot 10^6$ Pa pressure rating, 0.002 - 0.5 kg s^{-1} mass flow rate operating range, stainless steel with PFA liner, size DN8, 1/4" G screw end connections.	20600	1PC	20600
PG1, PG2, PG3, PG4	WIKA	Bourdon tube pressure gauge, cleaned for GOx use, 100 mm display, 0 - $60 \cdot 10^6$ Pa pressure display range, $60 \cdot 10^6$ Pa pressure rating, stainless steel, 3/8" G screw end connection.	1285	4PC	5140
PS5, PS8	Kistler	Piezoelectric pressure sensor, type 603CA-A, 0 - $100 \cdot 10^6$ Pa pressure range, charge (PE) output, acceleration compensated, stainless steel.	10656	2PC	21312

Continued on next page.

Table A.1 – continued from previous page.

Component(s)	Supplier	Selected unit	Unit price	Quantity	Cost
PS1, PS2, PS3, PS4, PS6, PS7, PS9	Kistler	M6 absolute pressure transmitter, type 4080B130, piezoresistive, $0 - 13 \cdot 10^6$ Pa pressure range, stainless steel.	11745	7PC	82215
TS1, TS3, TS4	Minco	Resistance temperature detecting immersion type probe, part S604PD40Z120, -269 - 260 °C measuring range, $10.3 \cdot 10^6$ Pa pressure rating, stainless steel.	685	3PC	2055
TS2	DIAS Infrared Systems	High-resolution IR camera, PYROVIEW 768N protection model, 1673.15 - 3273.15 K temperature measurement range, 50 Hz measurement frequency, 40 ms response time, $39^\circ \times 30^\circ$ (Horizontal Field Of View (HFOV) x Vertical Field Of View (VFOV)) aperture angle, 768x576 pixel resolution video output, industrial protection housing IP65. Includes mounting accessories, system and Ethernet cables and PYROSOFIT Data AcQuisition (DAQ) software.	202572	1PC	202572
I/O Module	Red Lion	EtherTRAK-2 I/O Module, part E2-16AI-8AO-D, 16 analog input channels, 8 analog output channels.	10710	1PC	10710
PRELIMINARY TOTAL COST					1054801

Appendix B

Edge of Space combustion chamber



FIGURE B.1: Figures of a combustion chamber developed by Edge of Space. Image source: Edge of Space (via Dr. Élcio Jeronimo de Oliveira).